The CLAMP GA-binding transcription factor regulates heat stress-induced transcriptional repression by associating with 3D chromatin loops

Joseph Aguilera[1], Jingyue Duan[2], Kaitlyn Cortez[1], Rachel S. Lee[3], Angelica Aragon[1], Mukulika Ray[4*] and Erica Larschan[1*]

*Co-corresponding authors

mukulika_ray@umb.edu, erica_larschan@brown.edu

[1] MCB department, Brown University, Providence, RI, USA
[2] Cornell Animal Science, College of Agriculture and Life Sciences, Cornell University, Ithaca, NY, USA
[3]Duke University School of Medicine, Durham, NC, USA
4 Department of Biology, University of Massachusetts Boston, MA, USA

Abstract

To survive exposure to heat stress (HS), organisms activate stress response genes and repress constitutive gene expression, thereby preventing the accumulation of potentially toxic RNA and protein products. Although many studies have elucidated the mechanisms that drive HS-induced activation of stress response genes across species, little is known about the mechanisms that repress constitutively expressed genes. Using nascent RNA-sequencing, we determined that CLAMP (Chromatin-linked adaptor for MSL complex proteins) is a critical GA-binding transcription factor (TF) that drives 75% of the Heat shock (HS) induced repression in *Drosophila,* a well-established model for understanding the mechanisms of heat stress-regulated gene regulation. Using Micro-C, we demonstrate for the first time that heat stress induces widespread changes in local 3D chromatin organization at chromatin loops, which are significantly associated with HS-induced transcriptional changes. Furthermore, we demonstrate that CLAMP regulates 3D chromatin loop formation and HS-induced repression through both direct and indirect mechanisms. Overall, we demonstrate that CLAMP is the first sequence-specific transcription factor identified that targets HS-dependent transcriptional repression by suppressing 3D chromatin loop anchor formation during HS and also present the highest resolution heat stress 3D genomic dataset available in

Drosophila, which provides a key resource for generating mechanistic insight into how temperature regulates 3D genomic contacts.

Introduction

Understanding how external stimuli regulate gene expression is essential for reducing the effects of dynamic changes in abiotic factors on all living organisms. One such external stimulus, temperature, plays a vital role in determining viability and fertility, which often decrease as temperatures rise (1). Heat stress (HS) rapidly changes transcription of both heat stress genes, which become activated, and constitutive genes, which become repressed (2,3). Therefore, understanding the mechanisms that drive changes in transcription upon heat stress will provide critical insight into how transcription rapidly changes in response to stimuli. Because the heat stress response is rapidly inducible, many discoveries of fundamental transcriptional mechanisms have been made using this system, including pausing of RNA Polymerase II, which occurs at thousands of genes across species (4).

Heat stress induces two types of transcriptional changes: 1) activation of heat stress-induced genes; 2) repression of constitutively active genes (5). Best studied in *Drosophila*, decades of research have defined the mechanisms of heat stress-induced gene activation at heat shock-responsive genes, whose promoters contain specific DNA sequences called **H**eat **S**hock Elements (HSEs), bound by Heat Shock Factor (HSF) (4,6,7). In *Drosophila*, the GA-binding transcription factor GAF and transcription elongation factor NELF, which regulates RNA Polymerase II pause release, are also involved in heat stress-regulated gene activation (7-9). Furthermore, in mammals, NELF functions in HS-regulated transcriptional repression mediated by temperature-dependent phase transition (10). However, the mechanisms that target repression specifically to constitutively active genes remain unknown.

In contrast to activation, much less is known about the specific DNA-binding factors that target constitutive genes for repression after heat stress. Transcriptional repression involves a decrease in promoter-proximal paused RNA Polymerase II at repressed genes (3,7) and cryptic premature

termination of transcripts with impaired elongation rate and decreased processivity (10) (11). A report also suggests that heat stress induces the relocalization of architectural proteins from TAD borders to Polycomb binding sites at the interior of TADs, which changes 3D chromatin architecture to potentially regulate repression (12). However, the role of 3D chromatin architectural changes during the heat stress response still needs to be better understood, as another report suggests that global 3D architectural changes at the TAD and compartment levels do not occur upon heat stress (2). However, neither of these studies was conducted at a sufficiently high resolution to detect specific local 3D chromatin loop changes. Therefore, the mechanisms by which 3D chromatin changes regulate the heat stress response require further study.

Furthermore, HSF and GAF are involved in heat-stress-induced activation but not heat-stress-induced repression (7). GAF has context-dependent synergistic or antagonistic relationships with another GA-binding transcription factor, CLAMP (Chromatin-linked adaptor for MSL complex proteins) (13,14). Although these two transcription factors have similar GA-rich DNA recognition sequences, variation within seemingly similar *cis*-elements drives the context-specific targeting of CLAMP to the male X-chromosome and the histone locus, where it inhibits GAF binding (13,15). Additionally, CLAMP promotes long-range 3D chromatin interactions (16) and interacts with Negative Elongation Factor (NELF), which functions in heat shock repression (10,17). Therefore, we hypothesized that CLAMP regulates heat stress-induced transcriptional changes because it can directly compete for binding with GAF (13), which regulates heat shock activation, and CLAMP interacts with NELF, which regulates repression (17).

To test our hypothesis, we used three approaches: 1) nascent RNA-sequencing (SLAM-seq) to define the function of CLAMP in heat stress-induced transcriptional activation and repression; 2) Micro-C to identify CLAMP-dependent and independent genome-wide, high-resolution local changes in chromatin organization after heat stress, and 3) HiChIP to identify CLAMP-bound 3D chromatin loop anchors associated with heat-stress-dependent transcriptional regulation. We found that, unlike GAF, CLAMP regulates heat-stress-induced transcriptional repression at many more genes than activation, with 75% of all repression being CLAMP-dependent. The canonical heat stress-activated genes remain activated in the absence of CLAMP.

Furthermore, we demonstrate that heat stress induces global changes in local 3D chromatin organization at chromatin loop anchors. We found that CLAMP typically inhibits the formation of 3D chromatin loops during heat stress when it is directly bound to loop anchors. Furthermore, changes at the 3D but not the 2D level regulate CLAMP-dependent gene repression in response to heat stress. In addition, prior to heat stress, we compared binding of different insulator proteins and chromatin remodelers at CLAMP-dependent HS-repressed genes, which are associated with: 1) direct CLAMP-dependent HS-induced Down Loops, 2) indirect CLAMP-dependent HS-induced Down Loops, and 3) HS-induced loop change independent. We found that CLAMP **directly** regulates HS-induced repression at loci at which insulator proteins Ibf1/2, ZIPIC, and the chromatin remodeler ISWI, but not Polycomb, are present; these factors are co-bound to genes located at anchors of CLAMP-bound chromatin loops prior to heat stress. In contrast, CLAMP also regulates repression **indirectly** at loci where it is not bound by either affecting local 3D chromatin loop formation or regulating transcription independent of 3D looping. Future studies are required to identify which factors regulate the indirect effects on 3D looping and transcription in the absence of CLAMP. Overall, we identify the first DNA-binding factor that directly regulates repression of hundreds of genes upon heat stress and define how it directly regulates repression through modulating 3D contacts. Furthermore, we report a key resource to study HS-induced chromatin 3D structural changes because we generate the highest resolution map to date of heat stress-induced 3D genomic contacts. By investigating the mechanistic details of HS-induced repression, we will enrich our overall understanding of how transcription repression is regulated in response to environmental cues in a cellular context.

Materials and methods

Fly strains and husbandry

Drosophila melanogaster fly stocks were maintained at 24°C on standard corn flour sucrose media. Fly strains used: *fkh-GAL4* (Bloomington, #78061), *UAS-CLAMPRNAi[val20]* (Bloomington, #57163). These were crossed to obtain the desired genotype, *fkh-GAL4>UAS-CLAMPRNAi*.

Cell culture

Kc cells were maintained at 25°C in Schneider's media supplemented with 10% Fetal Bovine Serum and 1.4X Antibiotic-Antimycotic (Thermofisher Scientific, USA). Cells were passaged every 3 days to maintain an appropriate cell density.

Polytene chromosome squashes and immunostaining after HS

Third instar larvae from undriven *UAS-CLAMPRNAi* and *fkh-GAL4>UAS-CLAMPRNAi* were incubated for 40 min at 37°C in a water bath inside a microfuge tube plugged with a soft plug (18) and dissected immediately to pull out the salivary gland. Polytene chromosome squashes were prepared using dissected salivary glands as previously described in Reider et al. 2017 (15). We stained polytene chromosomes with rabbit anti-CLAMP (1:1000, SDIX) and mouse anti-RNA pol II (1:500, ab817, Abcam) antibodies. For detection, we used all Alexa Fluor secondary antibodies against rabbit and mouse at a concentration of 1:200 and visualized slides at 40X on a Zeiss Axioimager M1 Epifluorescence upright microscope with the AxioVision version 4.8.2 software.

SLAM-seq

15 µg each of *clamp* dsRNA and GFP dsRNA were used for *clamp* RNAi and GFP RNAi (con), respectively, per T25 flask. Kc cells were incubated with dsRNA in FBS minus media for 45 minutes and allowed to grow in media supplemented with 10% FBS for 6 days before harvesting. dsRNA targeting *gfp* (control) and *clamp* for RNAi have been previously validated and described (19). PCR products were used as a template to generate dsRNA using the T7 Megascript kit (Ambion, Inc., USA), followed by purification with the Qiagen RNeasy kit (Qiagen, USA).

Two replicates of each for *clamp* RNAi and *gfp* RNAi, HS (Heat stress) samples, and four replicates each for *clamp* RNAi and *gfp* RNAi, NHS (NHS) samples were used for SLAM-seq. Just before harvesting, cells were either incubated in 4SU (4-thiouridine) provided with SLAMseq Anabolic Kinetics Module (Cat. No. 061.24, Lexogen) at RT or at 37°C for one hour in the dark as per the manufacturer's instructions. Cells were immediately harvested and the pellet was resuspended in 1 mL of Trizol (Invitrogen, USA). RNA isolated in the dark and S4U-labeled transcripts are alkylated with Iodoacteamide as per manufacturer instruction (SLAMseq Explorer and Kinetics Kit user guide, Lexogen). Resulting modified total RNA was used for downstream NGS library preparation using QuantSeq 3‘mRNA-Seq Library Prep Kit for Illumina (FWD) (Cat.

No. 015, Lexogen). Libraries sequenced in Illumina Hiseq 4000 with 150x2 bp pair-end sequencing. For analysis Read 2 for the pair-end sequencing was discarded while performing downstream analysis since quality of Read 2 is very low due to the poly(T) stretch at the beginning of Read 2. Data submitted to Gene Expression Omnibus (GSE253645).

Micro-C

Two replicates each for *clamp RNAi* and *gfp RNAi*, HS (Heat stress) samples and for *clamp RNAi* and *gfp RNAi*, NHS (NHS) samples were used for Micro-C. Kc cells ($2X10^6$) were incubated with 15 µg each of *clamp* dsRNA and GFP dsRNA (same as used for SLAM-seq experiment), used for *clamp RNAi* and *gfp RNAi* (con), respectively, per well of a 6-well plate in FBS minus media for 45 minutes and allowed to grow in media supplemented with 10% FBS for 6 days before harvesting. Before harvesting, HS (Heat stress) samples were incubated at 37°C for one hour. 3 × 10^6 cells were used per Micro-C reaction. Cells were aliquoted into 1.5 ml tubes, spun at 500g in a swinging bucket rotor for 5 minutes to pellet the cells, which were placed in -80 °C after removing the supernatant for 1 hour as per the manufacturer's protocol (Dovetail™ Micro-C Kit user guide version 2.0). Next, cells were thawed at RT, resuspended in 200 µL of 1X PBS (Thermo Fisher Scientific, 10010023), and crosslinked using 0.3M DSG and 37% formaldehyde as per the manufacturer's protocol (Dovetail™ Micro-C Kit user guide version 2.0). Dovetail™ Micro-C Kit (Catalog # 21006), the DovetailTM Library Module for Illumina (Catalog # 25004), and the primer set for NGS library preparation (DovetailTM Dual Index Primer Set #1 for Illumina, Catalog # 25010) were used for digestion, proximity ligation, library preparation, ligation capture, and amplification. Libraries were subjected to Illumina 150x2 bp pair-end sequencing with 80X coverage. Data submitted to Gene Expression Omnibus (GSE297379).

HiChIP

Kc Cells were allowed to grow to confluence and harvested. Before harvesting, HS (Heat stress) samples were incubated at 37°C for one hour. 10 × 10^6 cells were used per HiChIP reaction, and two replicates each for NHS (non-heat stress) and HS (Heat stress). Crosslinking was performed using 0.3M DSG and 37% formaldehyde as per the manufacturer's protocol (Dovetail™ HiChIP MNase Kit user guide). Dovetail™ HiChIP MNase Kit (Catalog # 21007), which includes the Dovetail Library Prep Kit and the primer set for NGS library preparation, was used for digestion,

lysate preparation, chromatin immunoprecipitation, proximity ligation, and library preparation. Rabbit anti-CLAMP (5µg/sample, SDIX) was used for the immunoprecipitation step. Libraries were subjected to Illumina 150x2 bp pair-end sequencing. Data submitted to Gene Expression Omnibus (GSE253644).

Computational analysis

a) SLAM-seq Analysis

The nf-core/slamseq (v1.0.0) pipeline was used to process and analyze the SLAM-seq data (20,21). The following parameters were used in the pipeline: -profile singularity, --genome BDGP6, --read_length 150, --trim5 12, --polyA 4, --multimappers true, --quantseq false, --endtoend false, --min_coverage 2, --var_fraction 0.2, --conversions 1, --base_quality 27, --pvalue 0.05, --skip_trimming false, --skip_deseq2 false. Adapter trimming was performed using Trim Galore (0.6.5). Conversion-aware mapping, alignment filtering, multimapper recovery, SNP calling, read quantification, gene-level quantification collapsing, QC stats, and result summarizations were all performed using SlamDunk (0.4.3)(20). Differentially expressed genes were then determined using DESeq2 (1.22.1).

b) Micro-C analysis

Micro-C raw data was analyzed using the HiC-Pro toolkit (3.1.0) with default parameters. Normalized contact maps deriving from HiC-Pro were converted to the cooler format using utility scripts (https://github.com/nservant/HiC-Pro/tree/master/bin/utils) in the HiC-Pro toolkit (3.1.0). Subsequently, the cooler contact maps for each condition were used to identify differential chromatin interactions using the HiCcompare library (1.24.0) in Bioconductor (3.18). Significant differential chromatin interactions ($P < 0.01$) were used in a range of analyses throughout the study. Differential loops within our statistical cutoff were visualized in a MA plot in Python (3.8) using matplotlib (3.7.5) and seaborn (0.13.2). Furthermore, the bedtools suite (2.31.0) was used to perform overlaps (bedtools pairtobed) with dm6 genes, determining the number of genes that were localized within loops and their anchors, respectively. The Mann-Whitney test was used to determine the statistical significance of differential loop sizes between our studied conditions.

Moreover, differential loops were visualized and compared with other datasets in the study using the coolbox API (0.3.9) (22).

c) HiChIP Analysis

HiChIP raw data was analyzed using the Dovetail genomics Hi-ChIP documentation (https://hichip.readthedocs.io/en/latest/index.html). Sequences were mapped to the dm6 genome using the Burrows-Wheeler Aligner (0.7.17) (23) passing the following arguments: mem, -5, -S, -P, -T0; default values were used for all other settings. Using the parse module of pairtools (0.3.0), valid ligation events were recorded; the following parameters were changed from default values: --min-mapq 40, --walks-policy 5unique, --max-inter-align-gap 30. PCR duplicates were removed using the dedup module of pairtools (0.3.0). Subsequently, the split module of pairtools was used to generate the final bam and pair files. The samtools (1.17) sort module was used to sort the bam files. To determine the quality of the proximity ligation events, scripts generated by the Dovetail Genomics team were utilized, which are deposited in the following GitHub repository (https://github.com/dovetail-genomics/HiChiP).

The cooler suite (0.9.3) (24) was used to generate contact maps from pair files, and the coolbox API (0.3.9) (22) was used to visualize the contact maps and bigwig tracks. To call loops, the flexible FitHiChIP tool (10.0) (25) was used as resolutions are easily adjustable, and it can detect different categories of 3D chromatin interactions. Furthermore, since FitHiChIP required 1D peaks from the same tissue and conditions, MACS2 (2.2.9.1) was used to call peaks on the Hi-ChIP data. Differential loops between conditions were determined using edgeR in custom scripts located in the FitHiChIP repository (https://github.com/ay-lab/FitHiChIP) and were visualized in a MA plot in Python (3.8) using matplotlib (3.7.5) and seaborn (0.13.2). Differential loops were visualized using APA plots with the coolpup.py (61) suite (1.0.0), displaying average signal over loop focal points. The central pixel within the APA plot is the central bin (2.5 kb), which contains the differential chromatin contact. The total size of the region displayed, including the central bin, is represented within the figures legends or within plot. Scores represented in the top left corners of the APA plot correspond to the central pixel intensity relative to the background. Furthermore, the bedtools suite (2.31.0) was used to perform overlaps (bedtools pairtobed) with dm6 genes, determining the number of genes that were localized within loops and their anchors, respectively.

The Mann-Whitney test was used to determine the statistical significance of differential loop sizes between our studied conditions.

d) Integration of Micro-C, HiChIP, and SLAM-seq datasets

To overlap Micro-C and HiChIP (3D genomics) with SLAM-seq (nascent RNA sequencing), we first had to transform the output of each technique into a mutually comparable format. Therefore, to analyze all three datasets, Micro-C and HiChIP differential loops were annotated with FlyBase genes, and SLAM-seq differential transcripts were converted to FlyBase genes. Micro-C and HiChIP differential loop anchors were annotated using a custom Python script and the bedtools suite (2.31.0). In addition, the entire loop span was annotated using the bedtools suite (2.31.0), collecting all FlyBase genes that were localized at the loop anchors and within the loop. Using this method, we derived gene lists from the differential loop analyses of Micro-C and HiChIP, which we could compare with the SLAM-seq differential gene lists. All overlaps presented were visualized using the matplotlib-venn (0.11.9) Python package, and Fisher's Exact test combined with FDR correction was used to determine statistical significance between all gene lists (**Table S1**). The coolbox API (0.3.9) (22) was used to visually compare all datasets in the study, observing differential contact maps, chromatin loops, ChIP signal, nascent RNA signal, and genes within a specified region.

e) ChIP-seq Analysis

Raw data (GSE118047, GSE30740, GSE36374, GSE36393, GSE54529, GSE63518, GSE80702, GSE89244)(12,26-33) was filtered using Trim Galore (0.5.0), then aligned to the dm6 genome using the mem module of the Burrows-Wheeler Aligner (0.7.17) with default settings. BigWig tracks were produced using the bamCoverage module in the deeptools suite (3.2.1) with the following parameters: --binSize 50, --normalizeUsing CPM, --extendReads 200, --exactScaling, --centerReads, --blackListFileName dm6-blacklist.bed. The respective BigWig tracks were visualized using the coolbox API (0.3.9) and the deeptools suite (3.2.1) over regions of interest.

Results

1. CLAMP is required for the repression of transcription in response to heat stress.

To understand how the CLAMP GA-binding transcription factor regulates transcription after heat stress, we performed high-throughput sequencing of nascent RNA in *Drosophila* Kc cells using Thiol (SH)–linked alkylation for the metabolic sequencing of RNA (SLAM-seq) (34). SLAM-seq quantifies nascent mRNA by measuring 4SU (4-thiouridine) incorporation as thymine-to-cytosine (T to C) conversions. Cells were incubated in 4SU either at room temperature (RT) for one hour (No heat stress, NHS) or at 37°C for one hour (Heat stress, HS), and then immediately processed to identify which mRNAs incorporated 4SU within the total mRNA pool. Next, we compared the mRNAs incorporating 4SU under HS and NHS conditions to determine which transcripts had increased levels after HS (activated genes) and which transcripts had reduced levels after HS (repressed genes) (padj ≤ 0.05 and fold change ≥ 1.5).

Consistent with a prior report (7), we identified a subset of transcripts that were activated (**N = 995**) and a larger subset that was repressed (**N = 3,547**) in control (*gfp RNAi)* cells after heat shock (HS) (**Figure 1A**). HS-activated transcripts encompass all known heat stress-responsive genes, including those for heat shock chaperone proteins (**Table S2a**). Much less is known about the mechanisms that mediate HS-induced repression compared to activation. We hypothesized that HS-induced repression is mediated by the CLAMP GA-binding protein TF because it is known to compete with GAF, which regulates heat-stress-induced activation (7,13). Since CLAMP also regulates X-chromosome dosage compensation in addition to global transcription in both males and females, we decided to examine the function of CLAMP during the heat stress response in the Kc female cell line, which does not undergo dosage compensation.

In the absence of heat stress (NHS), our validated *clamp* RNAi treatment (13,35,36) causes increased levels of 987 nascent transcripts and decreased levels of 246 nascent transcripts (**Figure S1A**). Therefore, CLAMP functions as a repressor more frequently than an activator in Kc cells before heat stress (**Figure S1A, Table S2b**). After HS, unlike control (*gfp RNAi)* cells (**Figure 1A, Table S2a**), in *clamp* RNAi-treated cells, we observed very little down-regulation of ongoing

transcription (**Figure S1B, Table S2c**), and a widespread increase in transcript levels in *clamp* RNAi-treated cells compared with control *gfp* RNAi-treated cells (**4,028** upregulated transcripts; **58** downregulated transcripts) (**Figure 1B, Table S2d**).

We also tested whether CLAMP promotes repression of heat stress response genes *in vivo*. We examined the distribution of active RNA Polymerase II (Pol II) on *Drosophila* larval salivary gland polytene chromosomes after HS (37°C) in control (undriven *clamp RNAi*) and salivary gland driver (*fkh-GAL4>clamp RNAi*) larvae (**Figure 1C**). Consistent with extensive prior work (18,37), heat stress restricts the binding of active Pol II (red) to specific cytological positions corresponding to HS-activated loci on control polytene chromosomes (**Figure 1C**). In contrast, after *clamp* RNAi, active Pol II (red) remains bound genome-wide, including at essential HS-activated loci, suggesting a loss of HS-induced repression but not activation. Notably, *clamp RNAi* flies retain CLAMP at the histone locus, consistent with prior reports (**Figure 1C**), perhaps because it contains 200 CLAMP binding sites (15). Overall, our data show that CLAMP is a stronger regulator of heat stress-induced repression than activation in both Kc cells and flies.

To determine whether CLAMP regulates HS-induced gene activation, we measured the effect of *clamp* RNAi on transcripts that were activated after HS in control cells (**Figure 1D**, **Table S2a, c**). We found that only 2.9 % (29 out of 995) of transcripts activated in control *gfp* RNAi cells are dependent on CLAMP (**Figure 1D**). In contrast, CLAMP inhibits further activation of 19% (190 out of 995) of HS-activated transcripts (**Figure 1D**). Furthermore, all well-studied canonical HS-induced transcripts, including the *hsp70* gene (7), are still induced even after *clamp* RNAi treatment (**Table S2d**). Next, we defined CLAMP-dependent HS repression by comparing HS-repressed transcripts (N=3547) with transcripts up-regulated in *clamp RNAi*-treated cells (N=4028) compared to control cells (*gfp RNAi*) under HS conditions (**Figure 1E**). We found that 75% (2660/3547) of the transcripts were CLAMP-dependently repressed after HS (**Figure 1E, Table S3**). Thus, *clamp* RNAi has a more substantial effect on HS-induced repression (75% of repressed transcripts are CLAMP-dependent, **Table S3**) than on activation (2.9% of activated transcripts are CLAMP-dependent, **Table S3**).

2. Heat stress induces widespread local 3D chromatin changes at chromatin loop anchors.

We next asked the question: How does CLAMP regulate transcriptional repression upon HS? Since heat stress induces aggregation of proteins and RNA, specially newly synthesized protein molecules (38), we predict that repression of ongoing transcription ensures that during heat stress the process of protein synthesis is inhibited at transcriptional level to aid the heat shock activation machinery consisting of protein chaperon that inhibit misfolding of synthesized protein and refolding of misfolded proteins. Thus, for all cell types with a cell-specific transcriptome, surviving under stress by conserving energy and preventing the formation of potentially toxic protein aggregates, the mechanism regulating repression of transcription upon heat shock (HS) needs to be essentially a global phenomenon. Therefore, we hypothesized that HS-induced global changes in transcription repression may be regulated by changes that have a genome-wide impact, such as global changes in 3D chromatin architecture. Additionally, CLAMP is known to regulate 3D chromatin loop formation and global changes in chromatin organization (16), which can be sensitive to changes in temperature, likely through phase transition (39), which CLAMP can undergo (40).

The function of 3D chromatin organization in the response to heat shock (HS) has remained unclear because the resolution of prior methods was low, and newer high-resolution techniques were not available when these experiments were conducted. One prior report suggests that HS induces the re-localization of architectural proteins from TAD borders to increase long-range interactions enriched with Polycomb marks, thereby regulating repression (12). In plants, HS alters the 3D arrangement of promoter-enhancer interactions to regulate the activation of heat shock-responsive genes (39,41,42). In contrast, other reports could not find a correlation between global three-dimensional chromatin changes and transcriptional changes after heat shock (2). Unfortunately, prior studies on 3D chromatin and HS used the HiC technique with a resolution of ~40 kb at anchor regions, making it challenging to understand the function of specific chromatin-associated factors that bind to approximately 0.1 kb. However, using the newer micro-C technique to measure 3D chromatin changes after HS, at a resolution of 1-5 kb, could make it possible to define local changes in chromatin organization marked by chromatin loops (43) that are regulated by a TF like CLAMP.

Thus, using the micro-C technique, we first investigated global changes in 3D chromatin loops at a resolution of 2.5kb after HS in control samples (*gfp RNAi*) identified those HS induced global changes in chromatin loops that were regulated by CLAMP by performing the micro-C method in *clamp* RNAi-treated cells under HS and NHS conditions (**Figure 2**). First, we identified widespread HS-induced changes in chromatin loops that were increased in frequency (Up loops, N= 24,291) and those decreased in frequency (Down loops, N = 4,265) by HS (**Figure 2A**). Interestingly, *clamp* RNAi enhanced HS induced loop formation (*clamp* RNAi HS Up-regulated Loops, N= 8,274) more frequently than it decreased HS induced loop formation (*clamp* RNAi HS Down-regulated Loops, N= 2,000). Thus, during heat stress, CLAMP primarily functions as an inhibitor of chromatin loop formation (**Figure 2B**).

Next, first we defined how genome-wide local 3D changes in chromatin loop formation correspond to gene distribution 1) within the chromatin loops and 2) at the loop anchors (**Figure 2C**), so that we can compare the chromatin-loop associated genes with CLAMP-dependent HS- HS-repressed genes (**Table S4**) to determine if HS-associated chromatin loop changes are related to HS-induced transcriptional repression. As expected at the loop anchors, which are 2.5 kb in length, on average, approximately one gene was associated within both HS-induced Up loops and Down loops with and without *clamp* RNAi because the average gene size is 3 kb in *Drosophila* (**Table S5**). However, when we evaluated the number of genes associated with each of these loop subcategories, we found significant differences across subcategories (**Figure 2C, Table S6**). HS-induced Down loops and *clamp* RNAi HS Down-regulated loops had ~3 genes within the chromatin loop span, compared to approximately one gene within the HS-induced Up loops and *clamp* RNAi HS Up-regulated loops (**Figure 2C**).

Next, we tested whether there were more genes in a loop because the loops were larger in length or because the genes were more densely packed within the same size loop (**Figure 2D**). For HS-induced chromatin loops, the HS-induced Down loops were significantly bigger (avg 626.54 kb) than HS-induced Up loops (avg 94.80 kb), and thus had more genes within the loop (**Figure 2C, D**). However, interestingly, the average size of both *clamp* RNAi HS Up-regulated and Down-regulated loops was significantly lower than that of control HS-induced chromatin loops,

indicating that CLAMP regulates the chromatin contacts that form shorter gene-rich loops. Furthermore, CLAMP regulates the majority (~85%) of all HS-associated changes in chromatin loops, and the majority of the time, it prevents their formation (**Figure 2E**).

After determining that CLAMP regulates HS-induced chromatin changes at gene-rich genomic regions, we asked whether these HS-associated 3D chromatin changes were related to HS-induced transcriptional changes (**Figure 2F-I**). We compared HS-regulated genes with genes located within (**Figures 2F-I**) and at loop anchors (**Figures S2A-D**) of the HS-induced chromatin loops. Since the latter comparison does not include all the genes associated with a chromatin loop, we have considered a list of genes within the identified chromatin loops in subsequent analysis to compare loop-associated genes with HS-induced transcriptionally regulated genes. Almost all HS-activated and HS-repressed genes overlapped with HS-induced loop changes (**Figures 2F and 2G**). This was unsurprising considering we identified whole-genome-wide chromatin loop changes induced by HS. However, we also found that most CLAMP-dependent HS-repressed genes (*clamp RNAi* HS Up-regulated genes) overlapped with *clamp* RNAi HS Up-regulated and Down-regulated loops (**Figures 2H and 2I**). Interestingly, most (**N=717, 68%**) of the CLAMP-dependent HS-repressed genes overlapped with HS loops suppressed by CLAMP (*clamp* RNAi HS Up-regulated loops) compared with HS loops promoted by CLAMP (**N=445, 42%**) (**Figures 2H-I).** Overall, these data are consistent with a function for CLAMP in repressing heat shock-induced gene expression by reducing the formation of chromatin loops that normally activate genes.

To further visualize the association of CLAMP-mediated chromatin loop changes with CLAMP-dependent HS-repression, we identified a 350 kb gene-dense region on chromosome 3L that is associated with a large number of HS-induced chromatin loops and multiple HS-repressed genes (**Figure 2J**). CLAMP regulates a subset of the chromatin loops in this region, and they are associated with CLAMP-dependent HS-repressed genes as well. Thus, we demonstrate that CLAMP regulates 3D chromatin changes during heat shock (HS), which are associated with CLAMP-dependent HS-induced transcriptional repression.

3. CLAMP inhibits chromatin loop formation during HS and regulates repression of associated genes

The next question we asked was whether CLAMP has a direct or indirect effect on 3D chromatin changes and related transcriptional changes after HS. High-resolution chromatin organization data in HS *clamp* RNAi cells reveal that CLAMP regulates chromatin loop rearrangement during HS (**Figure 2B**) at loops associated with CLAMP-dependent repressed genes (**Figure 2I, J**). However, to understand the direct role of CLAMP in transcriptional regulation after HS at high resolution in 3D, we used HiChIP to define which changes were directly associated with CLAMP binding to loop anchors. HiChIP measures TF binding and 3D loop anchors simultaneously at less than 1kb resolution (25,26,44), making it possible to define both TF binding and associated 3D chromatin loops. Therefore, we used HiChIP to investigate whether changes in 3D loop anchor contacts are associated with alterations in CLAMP occupancy on chromatin and HS-induced transcriptional repression.

We performed HiChIP using validated antibodies (15-17) targeting the CLAMP protein to identify CLAMP-associated loop anchors in Kc cells exposed to HS and matched control NHS Kc cells. Loop anchors bring distal regulatory elements closer to each other, which can regulate activation or repression of gene expression depending on the factors bound (26,45). Using the FitHiCHIP platform (25), we first identified CLAMP-bound chromatin loops (**Figure S3**): 1) present in control cells without HS (NHS) (**N=1515**); 2) shared loops that are present in both control (NHS) cells and HS cells (**N=421**); 3) loops present only after HS and not in NHS conditions (**N=563**). We then classified loops into subcategories based on whether they increased or decreased after heat shock: 1) CLAMP-bound HS induced Up loops and 2) CLAMP-bound HS induced Down loops gained upon HS (**Figure 3A, B**). We found that most CLAMP-bound chromatin loops are lost (**N=980, Down loops**) upon HS and very few are gained (**N=71, Up Loops**), clearly showing that CLAMP-bound chromatin loops are mainly down-regulated after HS. Our analysis shows that of the 980 CLAMP-associated HS induced down loops (HiChIP), 931 loops (95%) only had one anchor associated with CLAMP direct binding, while 49 loops (5%) had both anchors associated with CLAMP direct binding and of the 71 CLAMP-associated HS induced up loops (HiChIP), all

71 loops (100%) only had one anchor associated with CLAMP direct binding. Overall, we conclude that CLAMP promotes the loss of 3D chromatin loops at specific genomic locations after HS more frequently than it promotes the formation of new loops.

Next, we asked whether CLAMP changes its occupancy on chromatin when 3D loop contacts change. Therefore, we categorized CLAMP-bound loop anchors lost after HS (HS Down) and gained after HS (HS Up) into the following sub-classes depending on the change in occupancy of CLAMP on chromatin (similar to ChIP-seq) which HiChIP also quantifies in parallel with 3D loop anchors (**Figure S4**): 1) **H**igh **D**ifference (**HD**) in CLAMP occupancy between HS and NHS conditions; 2) **N**o **D**ifference (**ND**): <25% difference quantified by EdgeR (46,47) in CLAMP occupancy between HS and NHS conditions; 3) **L**ow **D**ifference (LD): >=25% difference quantified by EdgeR (46,47) in CLAMP occupancy between HS and NHS conditions. Because each loop has two ends, the loop anchors were further categorized into five types: HD-HD, HD-LD/ND, ND-ND, LD-ND, and LD-LD (**Figure S4A-F**). We found that most CLAMP-bound chromatin Up loop anchors (65/71: 92%) and Down loop anchors (849/980: 87%) upon HS belong to the ND or LD categories, in which CLAMP occupancy on chromatin is not dramatically changed. Thus, we conclude that upon HS, most CLAMP-bound chromatin changes occur through modulation of 3D chromatin contacts between loop anchors rather than through the gain or loss of CLAMP occupancy at specific genomic locations.

We also tested the average number of genes present, 1) at the loop anchors (**Table S7**) and 2) those within (**Table S8**) the CLAMP-bound HS-induced differential chromatin loops, along with the average loop length of CLAMP-bound loops. We found that CLAMP-bound loops were gene-rich, both at the loop anchors and within the loops, with average CLAMP-bound HS-induced chromatin loop sizes smaller (avg 37.58 kb) compared to global HS-induced differential loop size (**Figure 3C-D and Figure 2C-D**).

Since the majority of CLAMP-bound loops were down-regulated by heat shock, we investigated what proportion of global HS-induced Down-loops were CLAMP-bound chromatin loops and whether they overlapped with HS-repressed genes (**Figure 3E**). To determine how CLAMP-bound loops regulate gene expression, we also specifically tested if CLAMP-bound Down loops overlap

with CLAMP-dependent HS-repressed genes (**Figure 3F**). Interestingly, we also identified both CLAMP-dependent HS-repressed genes associated with CLAMP-bound chromatin loops lost after HS, and those that were associated with chromatin loops that were CLAMP-dependent, lost after HS but not direct targets of CLAMP (**Figure 3F**). Thus, we conclude that the repression of genes after HS due to changes in 3D chromatin architecture is both directly and indirectly regulated by CLAMP.

To visualize the types of loops that CLAMP mediates directly, we focused on a genomic region on chromosome 2R, where we identified a subset of global 3D chromatin loop changes directly bound and regulated by CLAMP (**Figure 3G**). We show that some CLAMP-bound chromatin loops are differentially affected by HS, and corresponding genes within these loops are repressed after HS. At the CLAMP-associated loops, before and after HS, there is no significant difference in CLAMP occupancy (**Figure 3G, V and VII**); however, there is differential chromatin loop formation, with a subset of Chromatin loops getting lost while others formed after HS (**Figure 3G, VI and VIII**). The repression of these target genes is CLAMP-dependent, as shown by the nascent RNA tracks from HS and NHS control and *clamp* RNAi-treated cells (**Figure 3G, IX, X**). Therefore, we conclude that CLAMP inhibits 3D chromatin loop formation during HS at a subset of gene-rich genomic locations, resulting in their transcriptional repression.

4. Presence of insulator proteins at Clamp-bound HS-induced Down chromatin loops prior to heat shock genes repressed during HS

Next, we asked the question: What combination of chromatin-associated factors distinguishes CLAMP-dependent repressed genes after HS due to changes in 3D chromatin architecture, directly and indirectly regulated by CLAMP? To address this question, we screened publicly available architectural protein datasets (GSE11804, GSE30740, GSE36374, GSE36393, GSE54529, GSE63518, GSE80702, GSE89244) (12,26-33), which were previously used to examine Pipsqueak (also, a GA-binding transcription factor similar to CLAMP) and Polycomb in 3D chromatin organization (26), to measure the occupancy of known chromatin marks and binding factors prior to HS at the CLAMP-dependent HS-repressed genes (N=735), which are associated

with: 1) direct CLAMP-dependent HS-induced Down-loops (N=106), 2) indirect CLAMP-dependent HS-induced Down-loops (N=388), and 3) HS-induced loop change independent (N=217) (**Figure 4A, B, and Table S9**). The first gene category comprises repressed genes directly regulated by CLAMP at the 3D chromatin organizational and transcriptional level after HS. In contrast, the second gene group is indirectly regulated by CLAMP at the 3D chromatin organizational level after HS, whereas the last group is regulated by CLAMP at only the transcriptional level and not the 3D chromatin organizational level (**Figure 4A, B**). 22% of CLAMP-dependent differential HS loops were associated with CLAMP directly, while the remaining 78% were indirectly affected by CLAMP (**Figure 4A**).

We identified factors present before HS at the CLAMP-dependent genes associated with CLAMP-bound chromatin loops and those associated with CLAMP-independent chromatin loops to understand the role of chromatin-associated factors involved in directly regulating HS-induced transcription repression by CLAMP. We used a set of random genes not repressed after HS as a control (**Figure 4C**). Genes in all three categories lacked repressive markers such as Su (Hw) and Pc (26,48) (**Figure 4C**). However, the CLAMP-dependent repressed genes associated with direct CLAMP-dependent HS-induced Down-loops were enriched for the CP190 interacting insulator binding factors (Ibf1 and Ibf2) (49) (**Figure 4C, D**). All CLAMP-dependent repressed genes had CP190, ZIPIC (Zinc-finger protein interacting with CP190), a promoter-bound TF with architectural and insulator function (49-52), and ISWI, a chromatin regulator (53) enriched at their TSS and TES (transcription start and end) sites, in NHS (Non Heat shock) cells compared to a random set of genes (**Figure 4C, D**). Thus, we hypothesize that Ibf1 and Ibf2 are important co-players that regulate repression of genes after HS directly by changes in 3D chromatin arrangement by CLAMP.

The presence of chromatin modeler-like ISWI and insulator proteins like ZIPIC and CP190 at these genes prior to HS suggests that, prior to heat stress, these genes are in a genomic region primed for transcription repression. During HS, CLAMP is responsible for the loss of the chromatin 3D loop structure at a subset of these sites with Ibf1/2, which facilitates the repression of transcription. On the other hand, genes enriched for ZIPIC and CP190, but lacking Ibf1/2 and CLAMP at the chromatin loops, still undergo 3D chromatin loop loss and repression after HS,

although CLAMP is not directly responsible for 3D chromatin loop changes. There must be other partner proteins that regulate changes in 3D chromatin organization and transcriptional repression at the later sites. Also, the last category of CLAMP-dependent repressed genes (**Figure 4B, C**) that are not associated with any 3D chromatin changes, do not show enrichment for any of the above factors compared to genomic regions undergoing 3D changes. How CLAMP regulates repression at these genes needs further investigation.

Overall, our studies have identified CLAMP as a critical DNA-binding factor associated with 3D chromatin loops that drives HS-dependent repression more frequently than HS-dependent activation. Our data are also consistent with a model in which CLAMP-regulated inhibition of chromatin loop formation after HS is responsible for repression of genes after HS (**Figure 5**). Future work must define the combinatorial context-specific interactions between all the factors we identified and other unknown factors determining whether a gene will become repressed upon heat stress due to 3D chromatin changes directly regulated by CLAMP or other unknown factors.

Discussion

Temperature is one important abiotic regulator of gene expression that substantially regulates biological functions. Defining how increasing temperature affects gene transcription has not only identified new transcriptional mechanisms but is vital for managing the effects of global changes in temperature on living organisms, including humans, plants, and other animals.

To survive under heat stress, cells must repress the ongoing transcription of constitutive gene transcripts to avoid accumulating toxic protein products, which would lead to cell death. Compared with decades of work on transcriptional activation upon heat stress (3-5,7), very few reports have provided insight into how HS-induced transcriptional repression is regulated (3,7,10-12,54). In particular, sequence-specific DNA-binding TFs that target genes for transcriptional repression remained unknown.

Here, we demonstrate that the GA-binding transcription factor CLAMP regulates the repression of approximately 75% of genes repressed upon heat stress. In contrast, CLAMP does not regulate any of the canonical genes activated upon heat stress, such as the heat shock protein genes (**Figure 1, Table S1a-d**). Furthermore, we found that HS results in genome-wide rearrangement of 3D chromatin structure at the local level of chromatin loops containing several genes. The CLAMP-bound 3D chromatin loops that are lost upon heat stress are associated with repressed genes, suggesting that local changes in 3D genome organization regulate transcription upon HS. However, the loss of CLAMP-associated loop anchors alone is insufficient to determine whether a gene will be activated or repressed because CLAMP-associated loop anchors are lost upon HS at both repressed and activated genes (**Figure 2**).

All CLAMP-dependent HS-repressed genes are modestly enriched for ZIPIC, a zinc finger protein, prior to HS. ZIPIC is an architectural protein with homodimerization domains that promotes CP190-mediated insulator activity and boundary formation, which can prevent transcription of nearby genes (50-52), another protein modestly enriched at the CLAMP-dependent HS-repressed genes. CLAMP physically interacts with CP190 and both promote gypsy chromatin insulator activity (55). Also, most (67%) CLAMP-dependent HS-repressed genes are associated with HS-dependent chromatin loop changes regulated by CLAMP, either directly or indirectly (**Figure 4A**). We found that CLAMP-dependent HS-repressed genes at which CLAMP directly regulates chromatin looping were enriched for the Ibf1/2, insulator proteins interacting with CP190 (49) (**Figure 5**). However, future work is necessary to define the CLAMP interacting factors at loci where CLAMP indirectly regulates 3D chromatin changes during HS without binding to the loop anchors, as well as at the smaller group of loci where HS-induced transcriptional repression is loop-independent. Furthermore, how the combinatorial context-specific interactions between all the factors we identified and other unknown factors determine whether a gene will become repressed upon heat stress still needs to be understood.

Also, we have not yet determined how HS results in 3D chromatin changes at CLAMP-bound loops, especially in places where there is no concurrent loss in CLAMP occupancy after HS. We predict that loss of the loop after HS would result in transcriptional repression due to loss of interactions that activate transcription through 3D looping or 2D mechanisms such as RNA

Polymerase II pause release (7). Also, we show that the direct effect of CLAMP on chromatin looping to mediate repression is associated with binding prior to HS of the insulator chromatin factors (Ibf1/2) and not the Polycomb and Su(Hw) complexes. However, it is possible that after heat stress, the occupancy of these factors changes, and the biophysical mechanisms by which CLAMP and Ibf 1/2 drive 3D chromatin structural changes remain unclear.

CLAMP is an intrinsically disordered protein with a prion-like domain, PrLD (13,40). Therefore, we speculate that heat stress may result in biophysical changes at CLAMP-associated loop anchors that regulate the liquid-liquid phase separation properties of bound proteins. We have recently shown that CLAMP itself can undergo a phase transition (40). Several reports suggest that increases in temperature influence phase separation properties of disordered proteins with prion-like domains (PrLD) (10,56-60). Therefore, it is possible that HS induces changes in the phase separation properties of CLAMP at the loop anchors. Also, CLAMP influences the recruitment of Negative Elongation Factor (NELF) that forms condensates under stress to drive transcriptional repression (10,17). In the future, it would be interesting to define how the CLAMP-NELF and CLAMP-Ibf interactions affect HS-induced transcriptional repression. The presence of a different combination of chromatin-bound factors at different CLAMP-bound target genes may regulate the phase transition properties of the locus, which could determine whether a gene will be activated or repressed upon HS. However, further experiments need to be done to test this hypothesis using *in vitro* chromatin models.

Overall, we show that the GA-binding TF CLAMP is a key DNA-binding factor that promotes transcriptional repression after HS more strongly than activation. Insight into transcriptional repression is important because the mechanism of HS-induced transcriptional repression has remained much less understood than HS-induced activation across species. We also generate new high-resolution 3D and gene expression data sets that can be used for developing combinatorial predictive models of how gene expression is rapidly modulated under different conditions. However, future work is necessary to define the combinatorial context-specific interactions between all of the factors we identified and other unknown factors that determine whether a gene will become activated or repressed upon heat stress.

Author contribution

M.R. and E.N.L. planned experiments, analyzed results, and wrote the manuscript. J.L.A., M.R., and K.C. performed micro-C experiments. M.R. and J.L.A. performed the HiChIP experiments. M.R. and J.D. performed the SLAM-seq experiments. J.D. performed computational analysis of the SLAM-seq data. J.L.A. and A.A. performed computational analysis of micro-C and HiChIP data, generated and integrated both data sets with available ChIP data sets, and generated SLAM-seq data sets. J.L.A. and J.D. reviewed and edited the manuscript. S.M.L. performed the polytene chromosome squashes and immunostaining after HS.

Conflict of interest

The authors declare no conflicting interests.

Funding

This work was supported by R35GM126994 to E.N.L. from NIH (National Institutes of Health). J.L.A. is funded by the HHMI Gilliam Scholar Program. S.M.L. was funded by Brown University's Undergraduate Teaching and Research Awards (UTRAs).

References

1. Richter, K., Haslbeck, M. and Buchner, J. (2010) The heat shock response: life on the verge of death. *Molecular cell*, **40**, 253-266.
2. Ray, J., Munn, P.R., Vihervaara, A., Lewis, J.J., Ozer, A., Danko, C.G. and Lis, J.T. (2019) Chromatin conformation remains stable upon extensive transcriptional changes driven by heat shock. *Proceedings of the National Academy of Sciences*, **116**, 19431-19439.
3. Mahat, D.B., Salamanca, H.H., Duarte, F.M., Danko, C.G. and Lis, J.T. (2016) Mammalian heat shock response and mechanisms underlying its genome-wide transcriptional regulation. *Molecular cell*, **62**, 63-78.
4. Guertin, M., Petesch, S., Zobeck, K., Min, I. and Lis, J. (2010), *Cold Spring Harbor symposia on quantitative biology*. Cold Spring Harbor Laboratory Press, Vol. 75, pp. 1-9.
5. Vihervaara, A., Duarte, F.M. and Lis, J.T. (2018) Molecular mechanisms driving transcriptional stress responses. *Nature Reviews Genetics*, **19**, 385-397.
6. Guertin, M.J. and Lis, J.T. (2010) Chromatin landscape dictates HSF binding to target DNA elements. *PLoS genetics*, **6**, e1001114.

7. Duarte, F.M., Fuda, N.J., Mahat, D.B., Core, L.J., Guertin, M.J. and Lis, J.T. (2016) Transcription factors GAF and HSF act at distinct regulatory steps to modulate stress-induced gene activation. *Genes & development*, **30**, 1731-1746.
8. Wu, C.-H., Yamaguchi, Y., Benjamin, L.R., Horvat-Gordon, M., Washinsky, J., Enerly, E., Larsson, J., Lambertsson, A., Handa, H. and Gilmour, D. (2003) NELF and DSIF cause promoter proximal pausing on the hsp70 promoter in Drosophila. *Genes & development*, **17**, 1402-1414.
9. Li, J., Liu, Y., Rhee, H.S., Ghosh, S.K.B., Bai, L., Pugh, B.F. and Gilmour, D.S. (2013) Kinetic competition between elongation rate and binding of NELF controls promoter-proximal pausing. *Molecular cell*, **50**, 711-722.
10. Rawat, P., Boehning, M., Hummel, B., Aprile-Garcia, F., Pandit, A.S., Eisenhardt, N., Khavaran, A., Niskanen, E., Vos, S.M. and Palvimo, J.J. (2021) Stress-induced nuclear condensation of NELF drives transcriptional downregulation. *Molecular cell*, **81**, 1013-1026. e1011.
11. Cugusi, S., Mitter, R., Kelly, G.P., Walker, J., Han, Z., Pisano, P., Wierer, M., Stewart, A. and Svejstrup, J.Q. (2022) Heat shock induces premature transcript termination and reconfigures the human transcriptome. *Molecular Cell*, **82**, 1573-1588. e1510.
12. Li, L., Lyu, X., Hou, C., Takenaka, N., Nguyen, H.Q., Ong, C.-T., Cubeñas-Potts, C., Hu, M., Lei, E.P. and Bosco, G. (2015) Widespread rearrangement of 3D chromatin organization underlies polycomb-mediated stress-induced silencing. *Molecular cell*, **58**, 216-231.
13. Kaye, E.G., Booker, M., Kurland, J.V., Conicella, A.E., Fawzi, N.L., Bulyk, M.L., Tolstorukov, M.Y. and Larschan, E. (2018) Differential occupancy of two GA-binding proteins promotes targeting of the drosophila dosage compensation complex to the male X chromosome. *Cell reports*, **22**, 3227-3239.
14. Duan, J., Rieder, L., Colonnetta, M.M., Huang, A., Mckenney, M., Watters, S., Deshpande, G., Jordan, W., Fawzi, N. and Larschan, E. (2021) CLAMP and Zelda function together to promote Drosophila zygotic genome activation. *Elife*, **10**, e69937.
15. Rieder, L.E., Koreski, K.P., Boltz, K.A., Kuzu, G., Urban, J.A., Bowman, S.K., Zeidman, A., Jordan, W.T., Tolstorukov, M.Y. and Marzluff, W.F. (2017) Histone locus regulation by the Drosophila dosage compensation adaptor protein CLAMP. *Genes & development*, **31**, 1494-1508.
16. Jordan, W. and Larschan, E. (2021) The zinc finger protein CLAMP promotes long-range chromatin interactions that mediate dosage compensation of the Drosophila male X-chromosome. *Epigenetics & Chromatin*, **14**, 1-16.
17. Urban, J.A., Urban, J.M., Kuzu, G. and Larschan, E.N. (2017) The Drosophila CLAMP protein associates with diverse proteins on chromatin. *PloS one*, **12**, e0189772.
18. Lakhotia, S.C., Mallik, M., Singh, A.K. and Ray, M. (2012) The large noncoding hsrω-n transcripts are essential for thermotolerance and remobilization of hnRNPs, HP1 and RNA polymerase II during recovery from heat shock in Drosophila. *Chromosoma*, **121**, 49-70.
19. Larschan, E., Soruco, M.M., Lee, O.-K., Peng, S., Bishop, E., Chery, J., Goebel, K., Feng, J., Park, P.J. and Kuroda, M.I. (2012) Identification of chromatin-associated regulators of MSL complex targeting in Drosophila dosage compensation. *PLoS genetics*, **8**, e1002830.
20. Neumann, T., Herzog, V.A., Muhar, M., von Haeseler, A., Zuber, J., Ameres, S.L. and Rescheneder, P. (2019) Quantification of experimentally induced nucleotide conversions in high-throughput sequencing datasets. *BMC bioinformatics*, **20**, 1-16.
21. Ewels, P.A., Peltzer, A., Fillinger, S., Patel, H., Alneberg, J., Wilm, A., Garcia, M.U., Di Tommaso, P. and Nahnsen, S. (2020) The nf-core framework for community-curated bioinformatics pipelines. *Nature biotechnology*, **38**, 276-278.
22. Xu, W., Zhong, Q., Lin, D., Zuo, Y., Dai, J., Li, G. and Cao, G. (2021) CoolBox: a flexible toolkit for visual analysis of genomics data. *BMC bioinformatics*, **22**, 1-9.

23. Li, H. and Durbin, R. (2009) Fast and accurate short read alignment with Burrows–Wheeler transform. *bioinformatics*, **25**, 1754-1760.
24. Abdennur, N. and Mirny, L.A. (2020) Cooler: scalable storage for Hi-C data and other genomically labeled arrays. *Bioinformatics*, **36**, 311-316.
25. Bhattacharyya, S., Chandra, V., Vijayanand, P. and Ay, F. (2019) Identification of significant chromatin contacts from HiChIP data by FitHiChIP. *Nature communications*, **10**, 4221.
26. Gutierrez-Perez, I., Rowley, M.J., Lyu, X., Valadez-Graham, V., Vallejo, D.M., Ballesta-Illan, E., Lopez-Atalaya, J.P., Kremsky, I., Caparros, E. and Corces, V.G. (2019) Ecdysone-induced 3D chromatin reorganization involves active enhancers bound by Pipsqueak and Polycomb. *Cell reports*, **28**, 2715-2727. e2715.
27. Wood, A.M., Van Bortle, K., Ramos, E., Takenaka, N., Rohrbaugh, M., Jones, B.C., Jones, K.C. and Corces, V.G. (2011) Regulation of chromatin organization and inducible gene expression by a Drosophila insulator. *Molecular cell*, **44**, 29-38.
28. Yang, J., Sung, E., Donlin-Asp, P.G. and Corces, V.G. (2013) A subset of Drosophila Myc sites remain associated with mitotic chromosomes colocalized with insulator proteins. *Nature communications*, **4**, 1464.
29. Kellner, W.A., Ramos, E., Van Bortle, K., Takenaka, N. and Corces, V.G. (2012) Genome-wide phosphoacetylation of histone H3 at Drosophila enhancers and promoters. *Genome research*, **22**, 1081-1088.
30. Van Bortle, K., Ramos, E., Takenaka, N., Yang, J., Wahi, J.E. and Corces, V.G. (2012) Drosophila CTCF tandemly aligns with other insulator proteins at the borders of H3K27me3 domains. *Genome research*, **22**, 2176-2187.
31. Van Bortle, K., Nichols, M.H., Li, L., Ong, C.-T., Takenaka, N., Qin, Z.S. and Corces, V.G. (2014) Insulator function and topological domain border strength scale with architectural protein occupancy. *Genome biology*, **15**, 1-18.
32. Cubenas-Potts, C., Rowley, M.J., Lyu, X., Li, G., Lei, E.P. and Corces, V.G. (2017) Different enhancer classes in Drosophila bind distinct architectural proteins and mediate unique chromatin interactions and 3D architecture. *Nucleic acids research*, **45**, 1714-1730.
33. Rowley, M.J., Nichols, M.H., Lyu, X., Ando-Kuri, M., Rivera, I.S.M., Hermetz, K., Wang, P., Ruan, Y. and Corces, V.G. (2017) Evolutionarily conserved principles predict 3D chromatin organization. *Molecular cell*, **67**, 837-852. e837.
34. Herzog, V.A., Reichholf, B., Neumann, T., Rescheneder, P., Bhat, P., Burkard, T.R., Wlotzka, W., Von Haeseler, A., Zuber, J. and Ameres, S.L. (2017) Thiol-linked alkylation of RNA to assess expression dynamics. *Nature methods*, **14**, 1198-1204.
35. Soruco, M.M., Chery, J., Bishop, E.P., Siggers, T., Tolstorukov, M.Y., Leydon, A.R., Sugden, A.U., Goebel, K., Feng, J. and Xia, P. (2013) The CLAMP protein links the MSL complex to the X chromosome during Drosophila dosage compensation. *Genes & development*, **27**, 1551-1556.
36. Urban, J., Kuzu, G., Bowman, S., Scruggs, B., Henriques, T., Kingston, R., Adelman, K., Tolstorukov, M. and Larschan, E. (2017) Enhanced chromatin accessibility of the dosage compensated Drosophila male X-chromosome requires the CLAMP zinc finger protein. *PloS one*, **12**, e0186855.
37. Teves, S.S. and Henikoff, S. (2011) Heat shock reduces stalled RNA polymerase II and nucleosome turnover genome-wide. *Genes & development*, **25**, 2387-2397.
38. Wallace, E.W., Kear-Scott, J.L., Pilipenko, E.V., Schwartz, M.H., Laskowski, P.R., Rojek, A.E., Katanski, C.D., Riback, J.A., Dion, M.F. and Franks, A.M. (2015) Reversible, specific, active aggregates of endogenous proteins assemble upon heat stress. *Cell*, **162**, 1286-1298.
39. Huang, Y., An, J., Sircar, S., Bergis, C., Lopes, C.D., He, X., Da Costa, B., Tan, F.-Q., Bazin, J. and Antunez-Sanchez, J. (2023) HSFA1a modulates plant heat stress responses

and alters the 3D chromatin organization of enhancer-promoter interactions. *Nature communications*, **14**, 469.
40. Ray, M., Zaborowsky, J., Mahableshwarkar, P., Vaidyanathan, S., Shum, J., Viswanathan, R., Huang, A., Wang, S.-H., Johnson, V. and Wake, N. (2024) Dual DNA/RNA-binding factor regulates dynamics of hnRNP splicing condensates. *bioRxiv*, 2024.2001. 2011.575216.
41. Sun, L., Jing, Y., Liu, X., Li, Q., Xue, Z., Cheng, Z., Wang, D., He, H. and Qian, W. (2020) Heat stress-induced transposon activation correlates with 3D chromatin organization rearrangement in Arabidopsis. *Nature communications*, **11**, 1886.
42. Liang, Z., Zhang, Q., Ji, C., Hu, G., Zhang, P., Wang, Y., Yang, L. and Gu, X. (2021) Reorganization of the 3D chromatin architecture of rice genomes during heat stress. *BMC biology*, **19**, 1-10.
43. Li, X., Tang, X., Bing, X., Catalano, C., Li, T., Dolsten, G., Wu, C. and Levine, M. (2023) GAGA-associated factor fosters loop formation in the Drosophila genome. *Molecular cell*, **83**, 1519-1526. e1514.
44. Mumbach, M.R., Rubin, A.J., Flynn, R.A., Dai, C., Khavari, P.A., Greenleaf, W.J. and Chang, H.Y. (2016) HiChIP: efficient and sensitive analysis of protein-directed genome architecture. *Nature methods*, **13**, 919-922.
45. Ogiyama, Y., Schuettengruber, B., Papadopoulos, G.L., Chang, J.-M. and Cavalli, G. (2018) Polycomb-dependent chromatin looping contributes to gene silencing during Drosophila development. *Molecular cell*, **71**, 73-88. e75.
46. Robinson, M.D., McCarthy, D.J. and Smyth, G.K. (2010) edgeR: a Bioconductor package for differential expression analysis of digital gene expression data. *bioinformatics*, **26**, 139-140.
47. Chen, Y., Lun, A.T. and Smyth, G.K. (2016) From reads to genes to pathways: differential expression analysis of RNA-Seq experiments using Rsubread and the edgeR quasi-likelihood pipeline. *F1000Research*, **5**, 1438.
48. Kahn, T.G., Savitsky, M., Kuong, C., Jacquier, C., Cavalli, G., Chang, J.-M. and Schwartz, Y.B. (2023) Topological screen identifies hundreds of Cp190-and CTCF-dependent Drosophila chromatin insulator elements. *Science Advances*, **9**, eade0090.
49. Cuartero, S., Fresán, U., Reina, O., Planet, E. and Espinàs, M.L. (2014) Ibf1 and I bf2 are novel CP 190-interacting proteins required for insulator function. *The EMBO journal*, **33**, 637-647.
50. Maksimenko, O., Bartkuhn, M., Stakhov, V., Herold, M., Zolotarev, N., Jox, T., Buxa, M.K., Kirsch, R., Bonchuk, A. and Fedotova, A. (2015) Two new insulator proteins, Pita and ZIPIC, target CP190 to chromatin. *Genome research*, **25**, 89-99.
51. Zolotarev, N., Fedotova, A., Kyrchanova, O., Bonchuk, A., Penin, A.A., Lando, A.S., Eliseeva, I.A., Kulakovskiy, I.V., Maksimenko, O. and Georgiev, P. (2016) Architectural proteins Pita, Zw5, and ZIPIC contain homodimerization domain and support specific long-range interactions in Drosophila. *Nucleic acids research*, **44**, 7228-7241.
52. Kaushal, A., Dorier, J., Wang, B., Mohana, G., Taschner, M., Cousin, P., Waridel, P., Iseli, C., Semenova, A. and Restrepo, S. (2022) Essential role of Cp190 in physical and regulatory boundary formation. *Science Advances*, **8**, eabl8834.
53. Dann, G.P., Liszczak, G.P., Bagert, J.D., Müller, M.M., Nguyen, U.T., Wojcik, F., Brown, Z.Z., Bos, J., Panchenko, T. and Pihl, R. (2017) ISWI chromatin remodellers sense nucleosome modifications to determine substrate preference. *Nature*, **548**, 607-611.
54. Goenka, A., Sengupta, S., Pandey, R., Parihar, R., Mohanta, G.C., Mukerji, M. and Ganesh, S. (2016) Human satellite-III non-coding RNAs modulate heat-shock-induced transcriptional repression. *Journal of cell science*, **129**, 3541-3552.

55. Bag, I., Dale, R.K., Palmer, C. and Lei, E.P. (2019) The zinc-finger protein CLAMP promotes gypsy chromatin insulator function in Drosophila. *Journal of cell science*, **132**, jcs226092.
56. Zhang, H., Shao, S., Zeng, Y., Wang, X., Qin, Y., Ren, Q., Xiang, S., Wang, Y., Xiao, J. and Sun, Y. (2022) Reversible phase separation of HSF1 is required for an acute transcriptional response during heat shock. *Nature cell biology*, **24**, 340-352.
57. Hutin, S., Kumita, J.R., Strotmann, V.I., Dolata, A., Ling, W.L., Louafi, N., Popov, A., Milhiet, P.-E., Blackledge, M. and Nanao, M.H. (2023) Phase separation and molecular ordering of the prion-like domain of the thermosensory protein EARLY FLOWERING 3. *bioRxiv*, 2023.2003. 2012.532276.
58. Dignon, G.L., Zheng, W., Kim, Y.C. and Mittal, J. (2019) Temperature-controlled liquid–liquid phase separation of disordered proteins. *ACS central science*, **5**, 821-830.
59. Chu, W.-T. and Wang, J. (2021) Thermodynamic and sequential characteristics of phase separation and droplet formation for an intrinsically disordered region/protein ensemble. *PLoS computational biology*, **17**, e1008672.
60. Chen, D., Lyu, M., Kou, X., Li, J., Yang, Z., Gao, L., Li, Y., Fan, L.-m., Shi, H. and Zhong, S. (2022) Integration of light and temperature sensing by liquid-liquid phase separation of phytochrome B. *Molecular Cell*, **82**, 3015-3029. e3016.

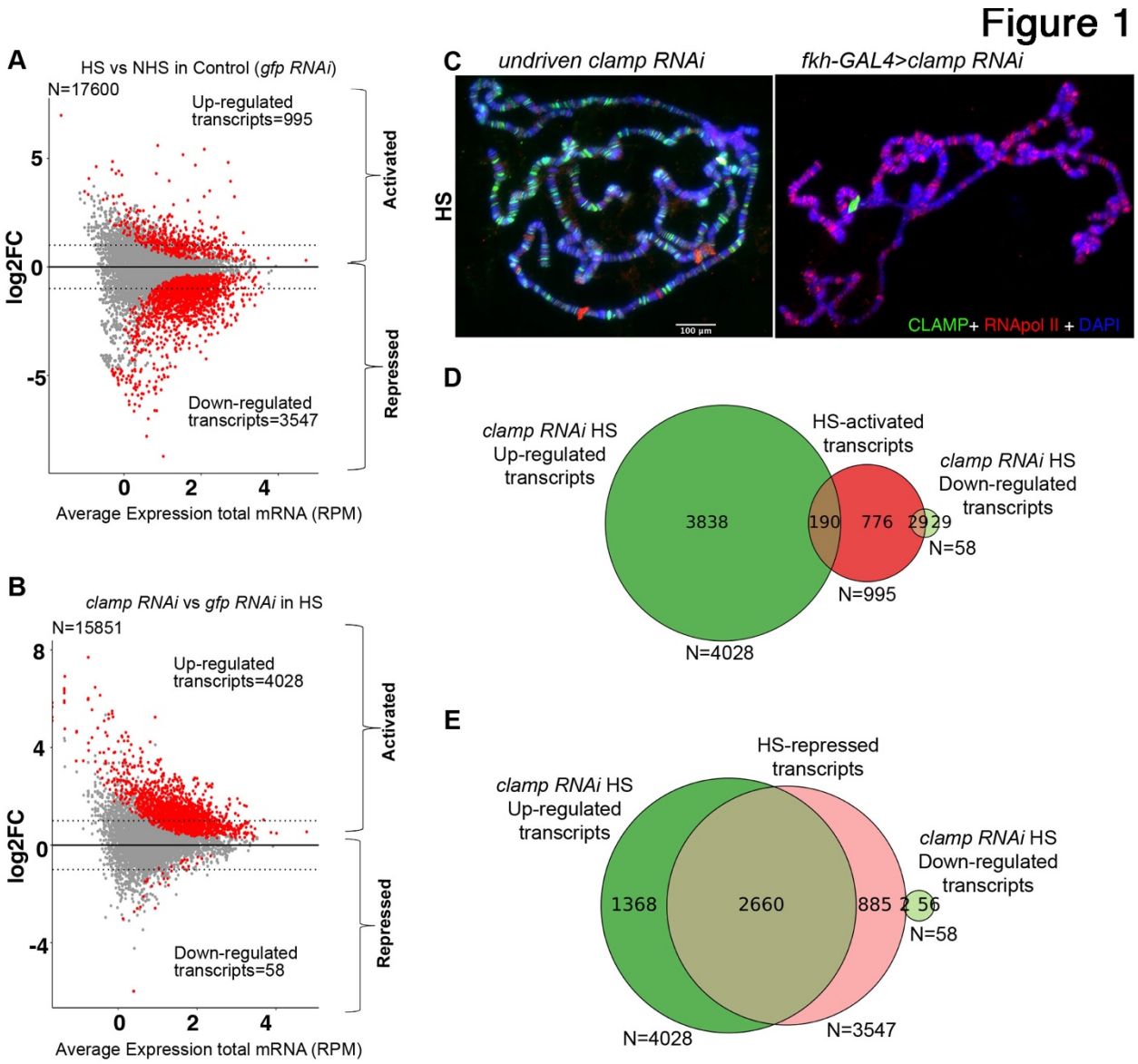

Figure 1. CLAMP regulates heat-stress-induced transcriptional repression more strongly than activation

A-B. MA plots showing significant changes (FC ≥ 1.5 and padj ≤ 0.05) in the levels of nascent transcripts (red dots) after HS (heat stress) compared to the control NHS (No heat stress) condition in control (*gfp RNAi*) cells (**A**) and after HS (heat stress) in the absence of CLAMP (*clamp RNAi*) compared to control (*gfp RNAi*) cells (**B**). Dotted horizontal lines in **A** and **B** denote ± 1 $\log_2$ FC change cutoffs.

C. Immunofluorescence images of HS (37ºC for 1 Hr) salivary gland polytene spreads showing the distribution of active RNA polymerase II (red) on chromatin (DAPI: blue) in the presence (undriven *clamp RNAi*) and absence (*fkh-GAL4>clamp RNAi*) of CLAMP (green). The scale bar (100 µM) applies to both panels in **C**.

D-E. Venn diagrams comparing HS-activated transcripts (deep red circle in **D**) and HS-repressed transcripts (light red circle in **E**) from control cells (*gfp RNAi*) to *clamp RNAi* HS Up-regulated (dark green circle) and *clamp RNAi* HS Down-regulated (light green circle) transcripts in *clamp* RNAi-treated cells.

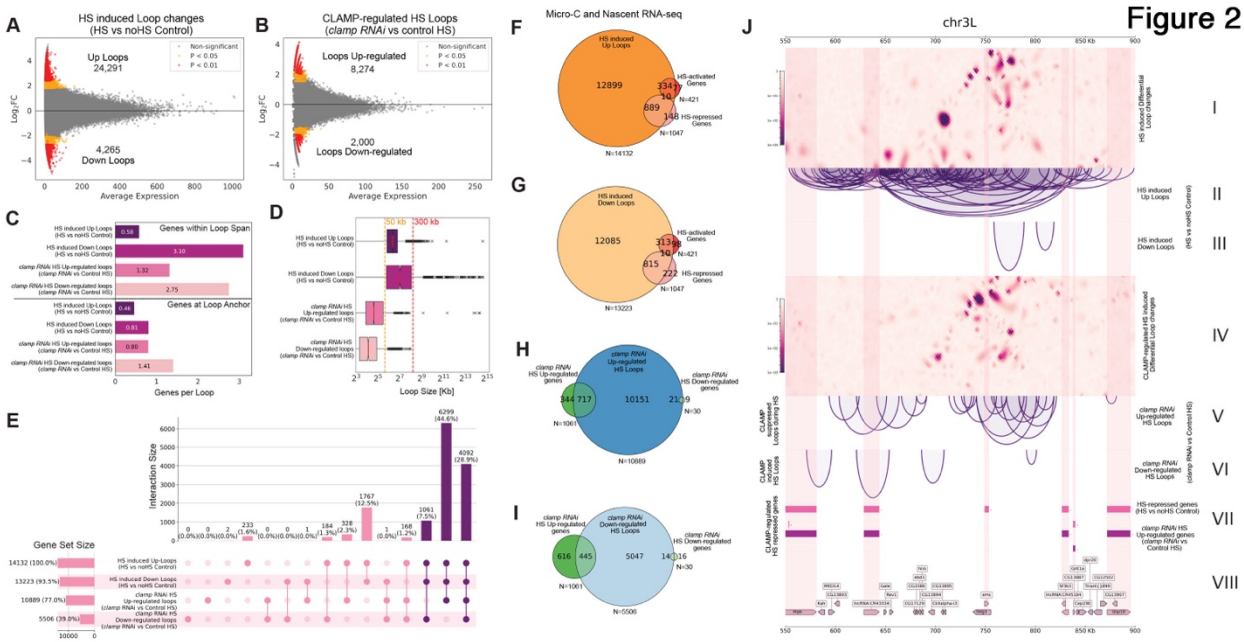

Figure 2. Heat stress induces widespread local 3D chromatin changes at the loop anchors

A-B. MA plots for **differential** loop anchors gained upon HS (HS induced Up loop anchors) or loop anchors lost upon HS (HS induced Down loop anchors) in control cells (**A,** Up loops=24,291, Down Loops=4,265**)** and *clamp RNAi* cells (**B,** Loops Up-regulated=8,274, Loops Down-regulated =2,000**). p<0.01**

C. Bar plots show the average number of genes associated with (top box) and present at (bottom box) the HS-induced genome-wide chromatin loop anchors and HS-induced CLAMP-dependent chromatin loop anchors.

D. Box plots showing average loop size of HS-induced genome-wide changing chromatin loops and CLAMP-dependent HS-induced differential chromatin loops with significant difference between average chromatin HS-induced up and down loop sizes, both in case of HS-induced genome-wide changing chromatin loops (Mann–Whitney Test, FDR corrected p=5.63E-186) and CLAMP-dependent HS-induced differential chromatin loops (Mann–Whitney Test, FDR corrected p=3.97E-70), and also between HS-induced genome-wide changing and CLAMP-dependent HS-induced differential chromatin loops themselves (Mann–Whitney Test, FDR corrected p=0)

E. Upset Plot showing genes associated with differential chromatin loop changes and cardinality of every category combination seen as chromatin loop changes after HS in control (top two rows) and *clamp* RNAi-treated (bottom two rows) cells. The first four columns show chromatin loop-associated genes only in each category, and the following six columns show those in each combination of exactly two named sets, the four columns after that combination of three named sets, and the last column shows genes associated with chromatin loop changes in all four categories. HS-associated CLAMP-dependent chromatin loop changes are mostly represented in the last three columns/bars.

F-I. Venn diagrams comparing HS-associated chromatin loop changes (genes within the loop) and HS-activated and repressed genes (**F** and **G**); as well as CLAMP-dependent chromatin loop changes during HS with CLAMP-dependent HS-induced transcriptional changes (**H** and **I**), showing significant (Fisher's Test) overlap between HS-associated Up loops (**F**) and Down loops (**G**) with HS-repressed genes; and CLAMP-dependent HS-associated Down loops (**H,** *clamp RNAi* up-regulated HS-loops) and Up loops (**I,** *clamp RNAi* down-regulated HS-loops) with CLAMP-dependent HS-repressed genes (*clamp RNAi HS* up-regulated genes). FDR corrected **p-values** are 7.487 E-09 (**F**), 2.53 E-4 (**G**), 2.0 E-6 (**H**), and 4.290 E-15 (**I**), respectively.

J. 350 kb region on 3L showing differential contact interaction results of selfish algorithm on HS and NHS micro-C contact map (**I**) with associated chromatin loops that are formed (**II**) and inhibited after HS (**III**). CLAMP-dependent differential contact interaction results of the selfish algorithm are shown on *clamp* RNAi-treated HS and control HS micro-C contact maps (**IV**) with

CLAMP inhibited (**V**) and favoured (**VI**) chromatin loops. The color bar in **I** and **IV** indicates the q-value (BH adjusted *p*-value) produced from the DCI analysis. Darker color means this interaction has a lower q-value; that is to say, two contact maps are more diverse at this location. Bed files for differential nascent RNA-seq (SLAM-seq) data from HS and NHS *clamp* RNAi-treated and control cells show the CLAMP-dependent HS-repressed genes (**VII**) among the corresponding genes within the genomic region associated with the loops (**VIII)**

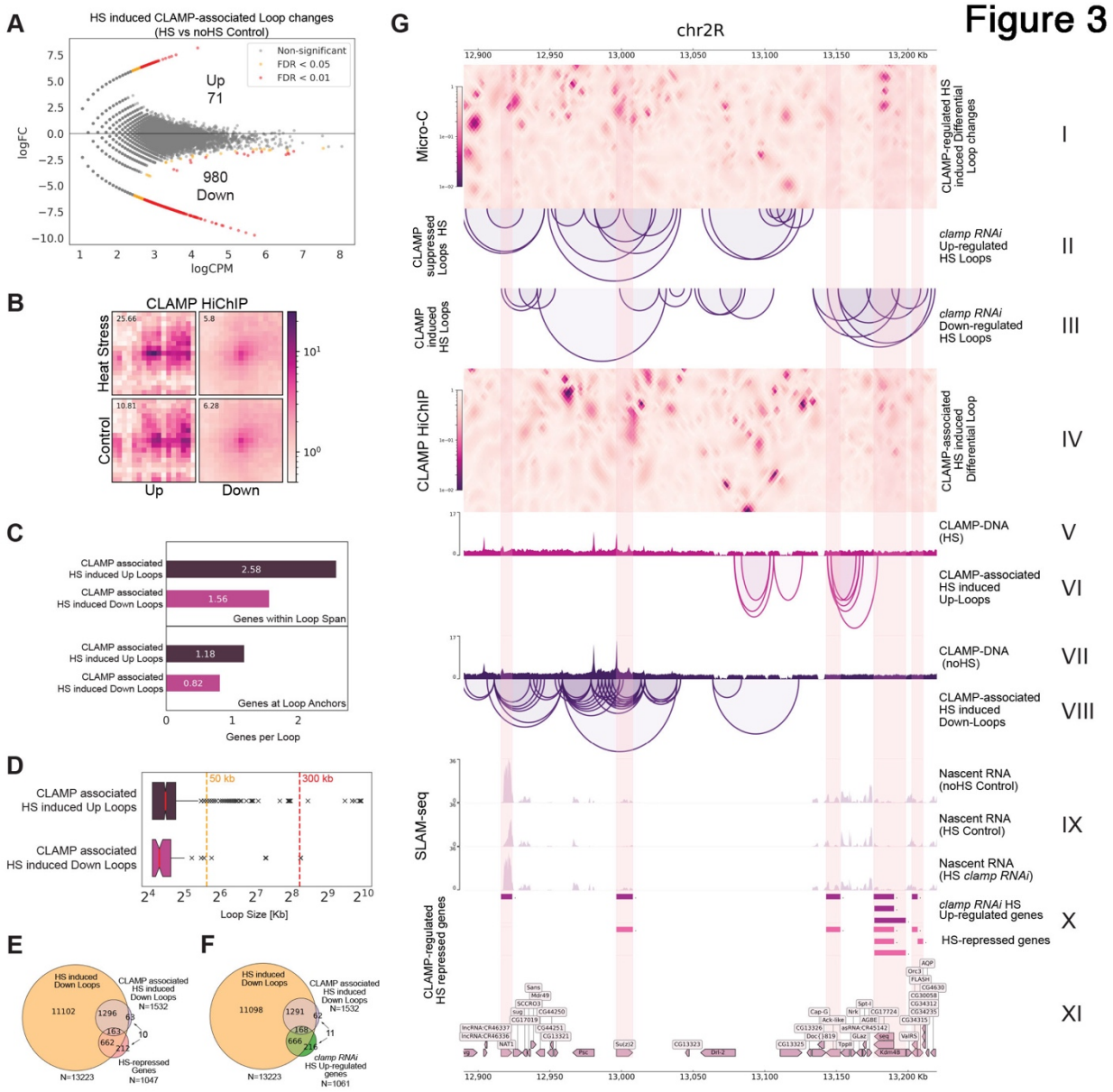

Figure 3. CLAMP regulates chromatin loop changes during HS, directly as well as indirectly, to repress gene transcription

A. 2D metaplot of CLAMP HiChIP data centered on significant interactions identified from CLAMP HiChIP under NHS or HS conditions for **differential** loop anchors gained upon HS (HS Up loop anchors, N=71) or loop anchors lost upon HS (HS Down loop anchors, N=980). The score indicates the enrichment of the center pixel compared with the top left corner.

B. CLAMP-bound loop pile-ups for HiChIP data from heat stress (HS) and control cells showing loss and gain of chromatin structures marked by chromatin loops defined in HS and control cells. The color is average interaction frequency across the entire dataset surrounding the defined HS Up and Down loops. A high signal indicates strong interaction between loop anchors. ±20 kb padding was applied to the central 2.5 kb bin, displaying a 42.5 kb aggregated region.

C. Barplots showing average number of genes associated within (top box) and present at (bottom box) the CLAMP-bound chromatin loop anchors up and down-regulated after Heat shock (HS)

D. Box plots showing significant difference (Mann–Whitney Test, FDR corrected p=0.0354) between average loop size of CLAMP-bound chromatin loop anchors up and down-regulated after Heat shock (HS).

E-F. Venn diagrams comparing all (Micro-C data) and CLAMP-bound (HiChIP data) chromatin loops lost after HS with HS-repressed (**E**) and CLAMP-dependent HS-repressed genes (**F**), showing significant (Fisher's Test) overlap between CLAMP-bound HS-associated Down-loops with global genome-wide loss of HS-associated loops (p=1.26E-115), HS-repressed genes (p=9.59E-18), and CLAMP-dependent HS-repressed genes (*clamp RNAi HS* up-regulated genes, p=2.57E-19).

G. 300 kb region on 2R showing CLAMP-regulated differential contact interaction results of selfish algorithm on *clamp* RNAi-treated and control HS micro-C contact map (**I**) with associated CLAMP suppressed (**II**) and induced (**III**) chromatin loops after HS. CLAMP-associated differential contact interaction results of the selfish algorithm are shown on HS and NHS CLAMP HiChIP contact maps (**IV**) with CLAMP-bound (**V** and **VII**) directly associated Up (**VI**) and Down (**VIII**) chromatin loops. The color bar in **I** and **IV** indicates the q-value (BH adjusted *p*-value) produced from the DCI analysis. Darker color means this interaction has a lower q-value; that is to say, two contact maps are more diverse at this location. Normalized reads and bed files for

differential nascent RNA-seq (SLAM-seq) data from HS and NHS *clamp* RNAi-treated and control cells show the CLAMP-dependent HS-repressed genes (**IX and X**) among the corresponding genes within the genomic region associated with the loops (**XI)**

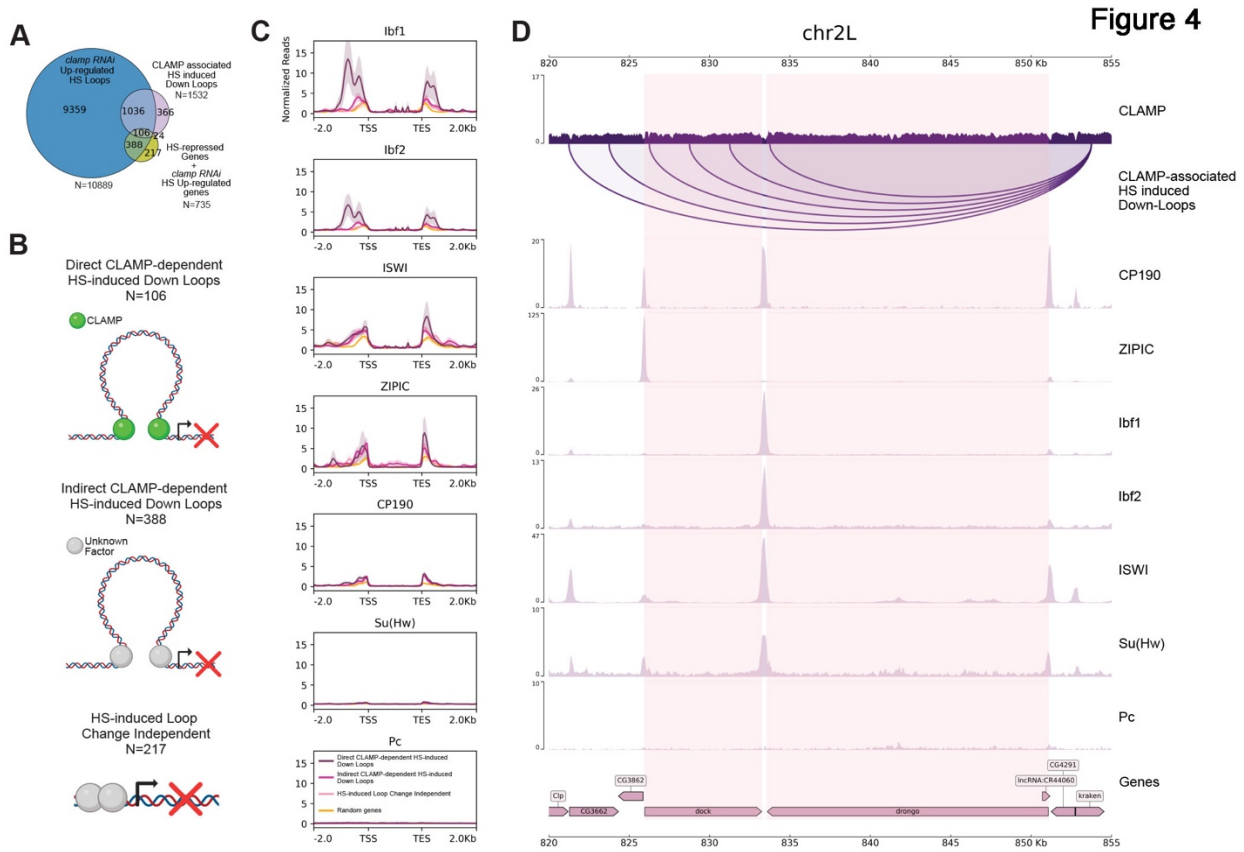

Figure 4. HS-associated chromatin loops directly and indirectly regulated by CLAMP have different chromatin-bound factors under NHS conditions

A. Venn diagram comparing all CLAMP-dependent (Micro-C data, *clamp RNAi* up-regulated HS Loops) and CLAMP-bound (HiChIP data) chromatin loops lost after HS with CLAMP-dependent HS-repressed genes, showing significant (Fisher's Test) number of CLAMP-dependent HS-repressed genes are associated with CLAMP-dependent loss of chromatin loops after HS (p=1.55E-04) and a significant proportion of these are directly CLAMP-bound (p=8.78E-32).

B. Schematic showing three categories of CLAMP-dependent HS-repressed genes based on 3D chromatin organisational changes associated with HS.

C. Average profile for chromatin-bound factors across CLAMP-dependent HS-repressed genes present at direct and indirect CLAMP-dependent HS-induced Down-loop anchors, genes not associated with any loop anchors, and a random set of genes (negative control).

D. 35 kb region on 2L showing distribution of chromatin bound factors at CLAMP-dependent HS-repressed genes *dock* and *drongo* and associated CLAMP-bound chromatin loops lost after HS

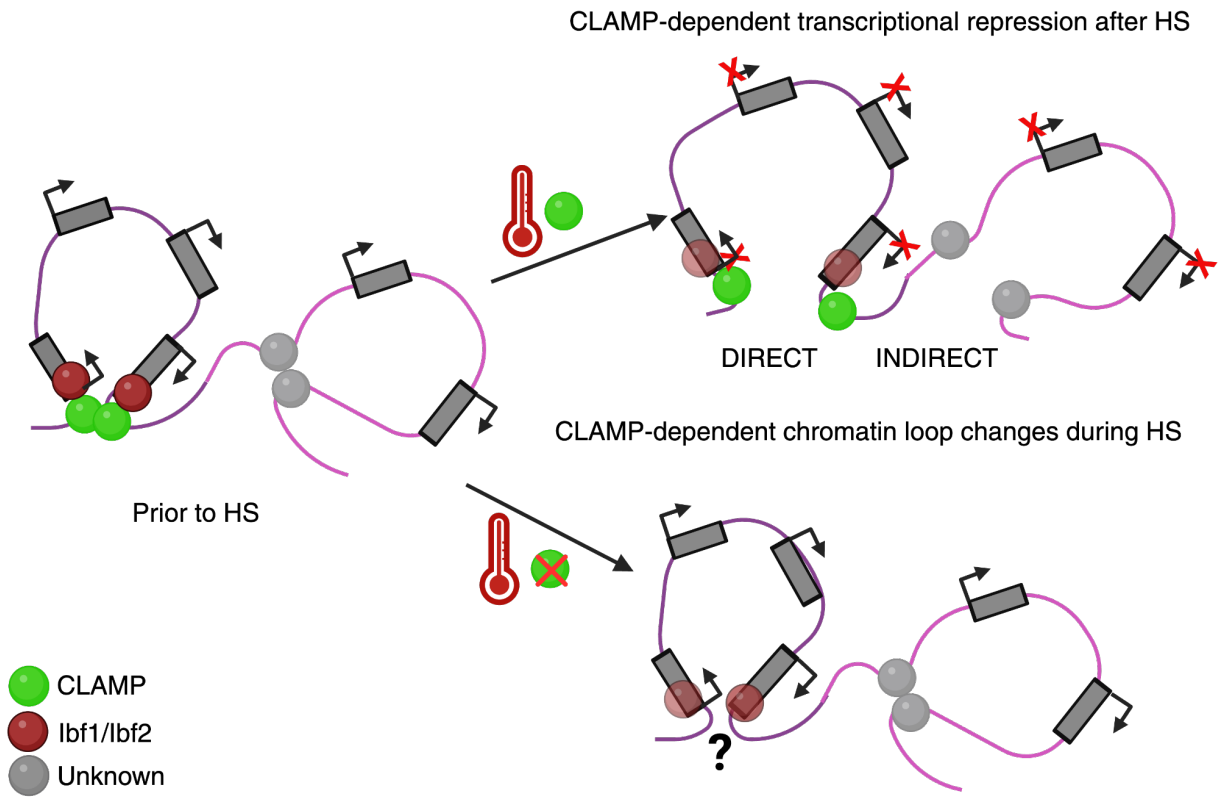

Figure 5. Model for CLAMP-dependent HS-induced transcriptional gene repression

Figure 1

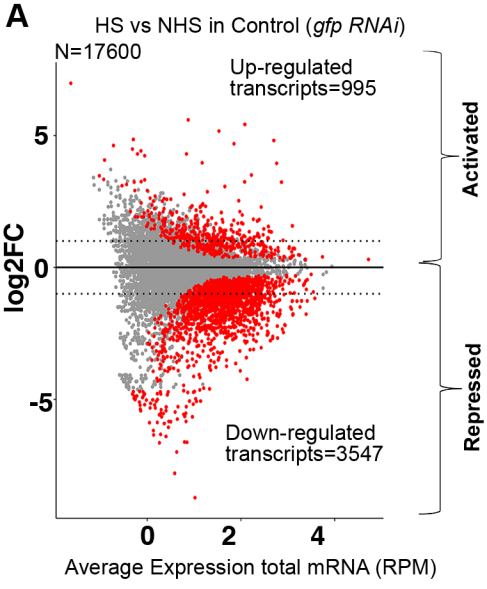
A
HS vs NHS in Control (gfp RNAi)
N=17600
Up-regulated transcripts=995
Down-regulated transcripts=3547
Activated
Repressed
log2FC
5
0
-5
0
2
4
Average Expression total mRNA (RPM)

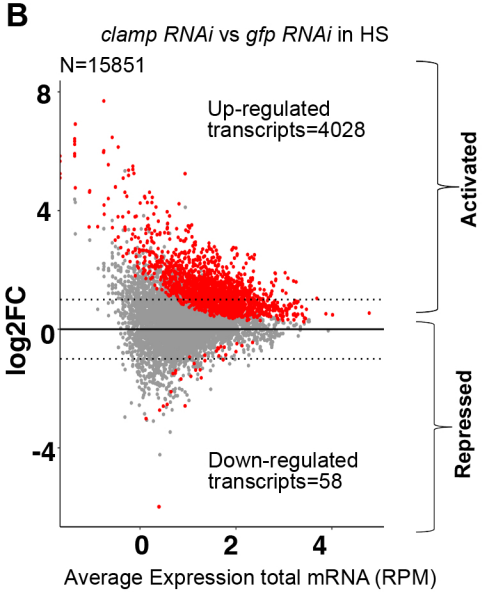
B
clamp RNAi vs gfp RNAi in HS
N=15851
Up-regulated transcripts=4028
Down-regulated transcripts=58
Activated
Repressed
log2FC
8
4
0
-4
0
2
4
Average Expression total mRNA (RPM)

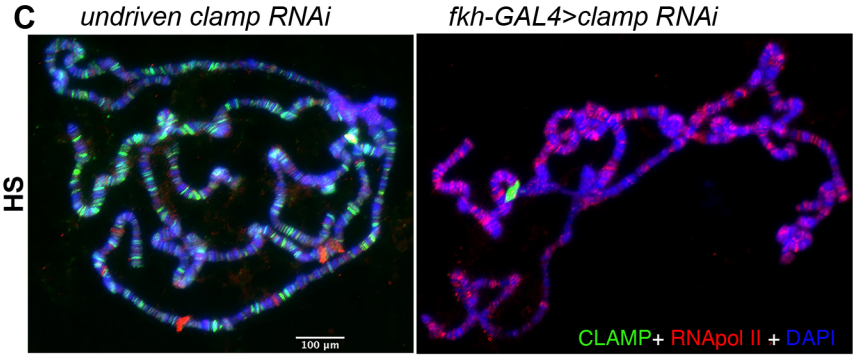
C
undriven clamp RNAi
fkh-GAL4>clamp RNAi
HS
100 µm
CLAMP+ RNApol II + DAPI

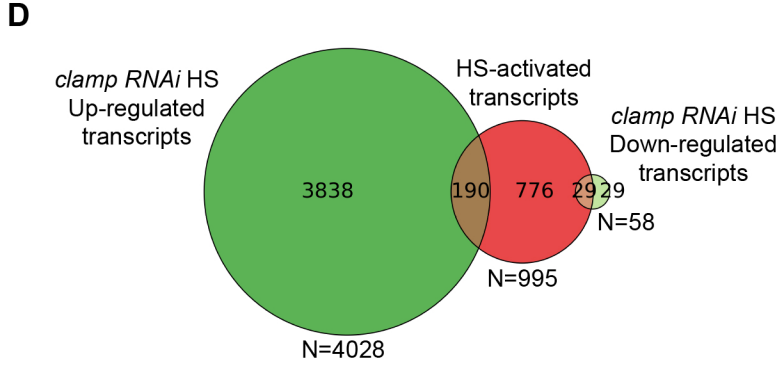
D
clamp RNAi HS Up-regulated transcripts
HS-activated transcripts
clamp RNAi HS Down-regulated transcripts
3838
190
776
29
29
N=58
N=995
N=4028

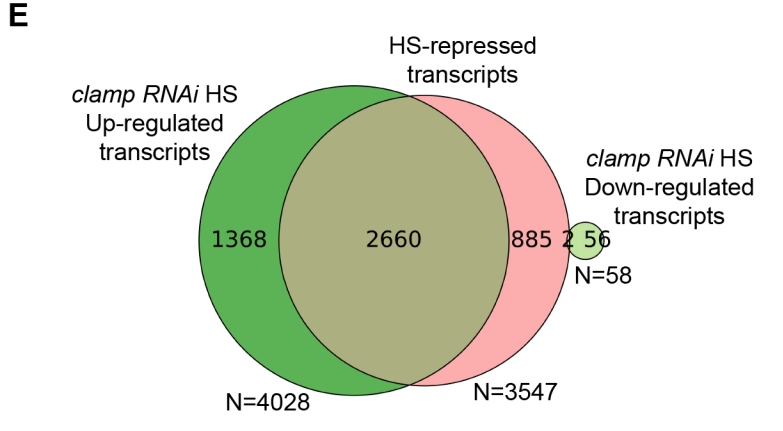
E
HS-repressed transcripts
clamp RNAi HS Up-regulated transcripts
clamp RNAi HS Down-regulated transcripts
1368
2660
885
2
56
N=58
N=4028
N=3547

Figure 2

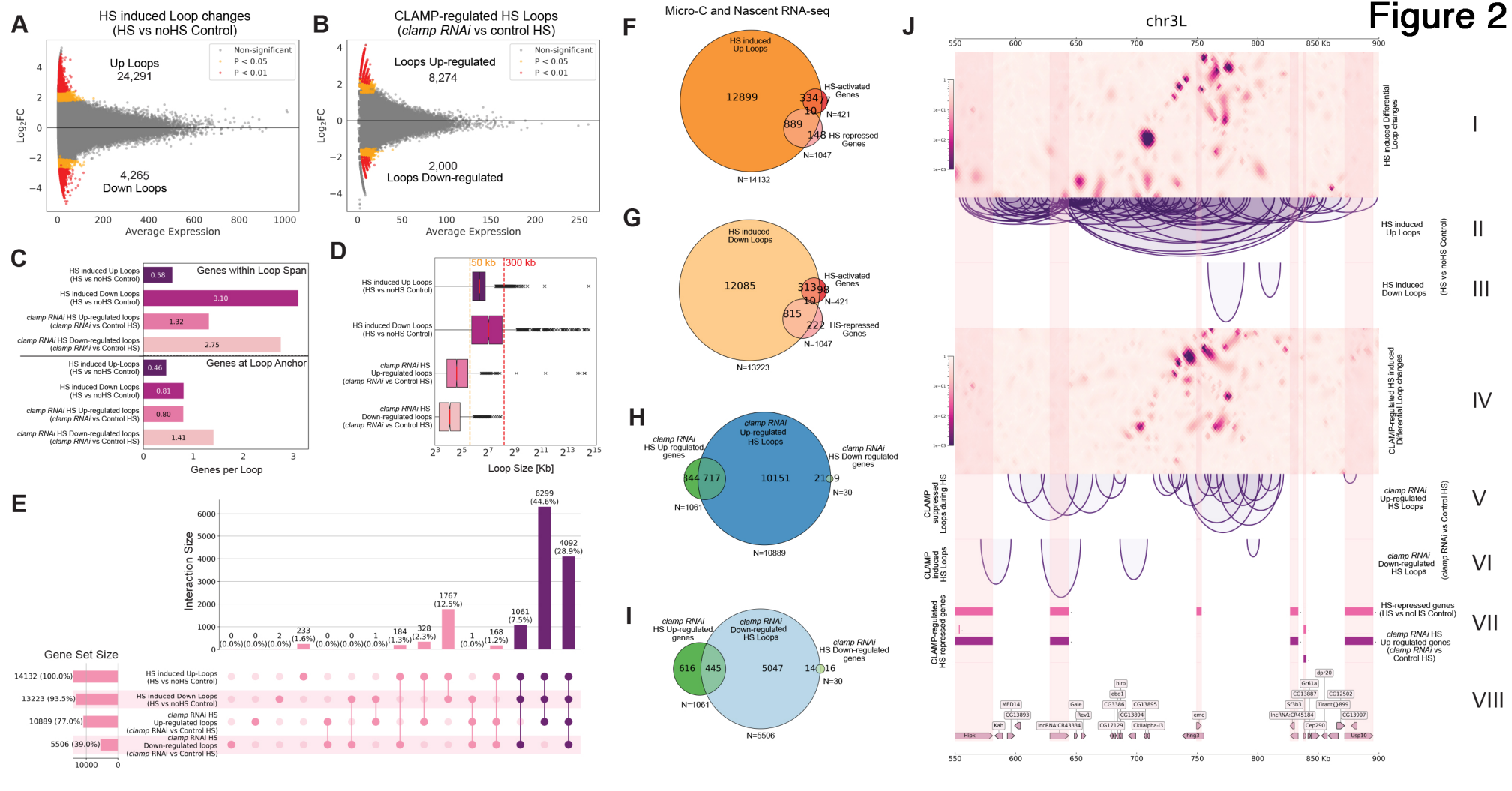
A
HS induced Loop changes
(HS vs noHS Control)
Up Loops
24,291
4,265
Down Loops
Non-significant
P < 0.05
P < 0.01
Log2FC
Average Expression
B
CLAMP-regulated HS Loops
(clamp RNAi vs control HS)
Loops Up-regulated
8,274
2,000
Loops Down-regulated
C
Genes within Loop Span
Genes at Loop Anchor
HS induced Up Loops (HS vs noHS Control)
HS induced Down Loops (HS vs noHS Control)
clamp RNAi HS Up-regulated loops (clamp RNAi vs Control HS)
clamp RNAi HS Down-regulated loops (clamp RNAi vs Control HS)
0.58
3.10
1.32
2.75
0.46
0.81
0.80
1.41
Genes per Loop
D
50 kb
300 kb
Loop Size [Kb]
E
Interaction Size
Gene Set Size
14132 (100.0%)
13223 (93.5%)
10889 (77.0%)
5506 (39.0%)
HS induced Up-Loops (HS vs noHS Control)
HS induced Down Loops (HS vs noHS Control)
clamp RNAi HS Up-regulated loops (clamp RNAi vs Control HS)
clamp RNAi HS Down-regulated loops (clamp RNAi vs Control HS)
6299 (44.6%)
4092 (28.9%)
1767 (12.5%)
1061 (7.5%)
Micro-C and Nascent RNA-seq
F
HS induced Up Loops
12899
3347
10
889
148
HS-activated Genes
N=421
HS-repressed Genes
N=1047
N=14132
G
HS induced Down Loops
12085
3139
8
10
815
222
HS-activated Genes
N=421
HS-repressed Genes
N=1047
N=13223
H
clamp RNAi HS Up-regulated genes
clamp RNAi Up-regulated HS Loops
clamp RNAi HS Down-regulated genes
344
717
10151
2109
N=30
N=1061
N=10889
I
clamp RNAi HS Up-regulated genes
clamp RNAi Down-regulated HS Loops
clamp RNAi HS Down-regulated genes
616
445
5047
1416
N=30
N=1061
N=5506
J
chr3L
HS induced Differential Loop changes
HS induced Up Loops
HS induced Down Loops
(HS vs noHS Control)
CLAMP-regulated HS induced Differential Loop changes
CLAMP suppressed Loops during HS
clamp RNAi Up-regulated HS Loops
CLAMP induced HS Loops
clamp RNAi Down-regulated HS Loops
(clamp RNAi vs Control HS)
CLAMP-regulated HS repressed genes
HS-repressed genes (HS vs noHS Control)
clamp RNAi HS Up-regulated genes (clamp RNAi vs Control HS)
I
II
III
IV
V
VI
VII
VIII

Figure 3

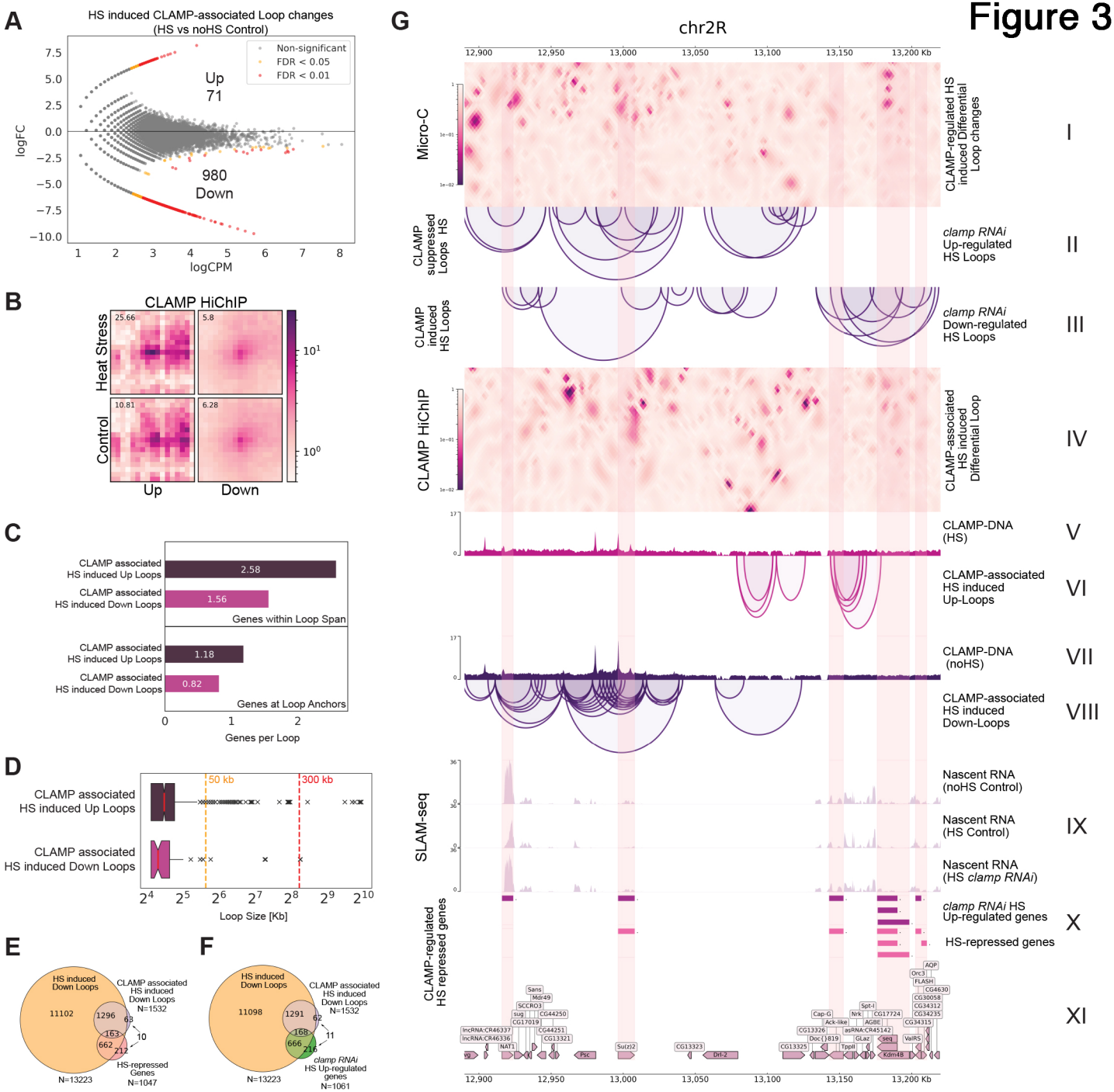
A
HS induced CLAMP-associated Loop changes
(HS vs noHS Control)
Non-significant
FDR < 0.05
FDR < 0.01
Up
71
980
Down
logFC
logCPM
B
CLAMP HiChIP
Heat Stress
Control
Up
Down
25.66
5.8
10.81
6.28
C
CLAMP associated HS induced Up Loops
CLAMP associated HS induced Down Loops
2.58
1.56
Genes within Loop Span
1.18
0.82
Genes at Loop Anchors
Genes per Loop
D
50 kb
300 kb
Loop Size [Kb]
E
HS induced Down Loops
CLAMP associated HS induced Down Loops N=1532
HS-repressed Genes N=1047
N=13223
11102
1296
63
163
10
662
212
F
HS induced Down Loops
CLAMP associated HS induced Down Loops N=1532
clamp RNAi HS Up-regulated genes N=1061
N=13223
11098
1291
62
168
11
666
216
G
chr2R
12,900
12,950
13,000
13,050
13,100
13,150
13,200 Kb
Micro-C
CLAMP-regulated HS induced Differential Loop changes
I
CLAMP suppressed HS Loops
clamp RNAi Up-regulated HS Loops
II
CLAMP induced HS Loops
clamp RNAi Down-regulated HS Loops
III
CLAMP HiChIP
CLAMP-associated HS induced Differential Loop
IV
CLAMP-DNA (HS)
V
CLAMP-associated HS induced Up-Loops
VI
CLAMP-DNA (noHS)
VII
CLAMP-associated HS induced Down-Loops
VIII
SLAM-seq
Nascent RNA (noHS Control)
Nascent RNA (HS Control)
IX
Nascent RNA (HS clamp RNAi)
CLAMP-regulated HS repressed genes
clamp RNAi HS Up-regulated genes
HS-repressed genes
X
XI

Figure 4

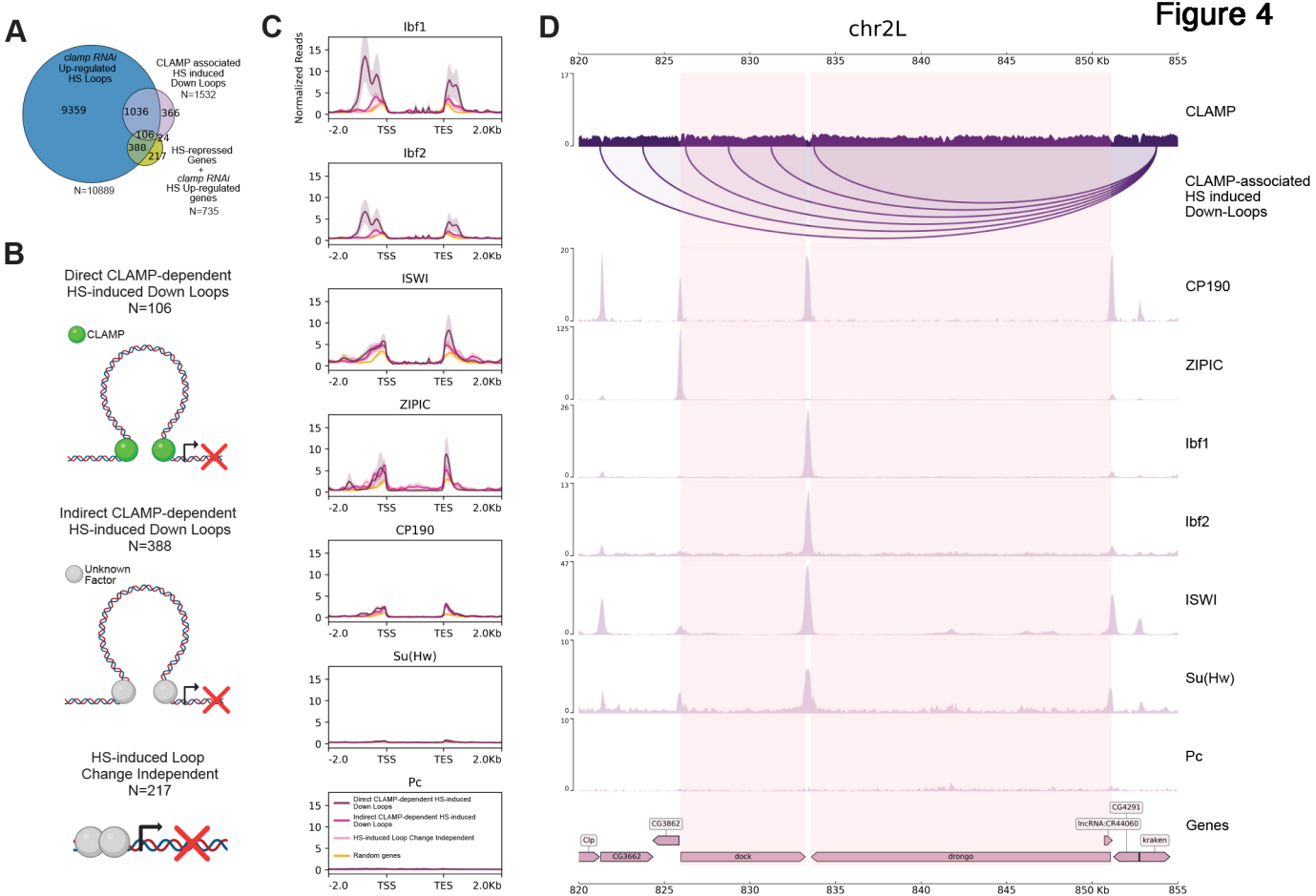
A
clamp RNAi Up-regulated HS Loops
9359
1036
366
106
24
388
217
N=10889
CLAMP associated HS induced Down Loops N=1532
HS-repressed Genes + clamp RNAi HS Up-regulated genes N=735
B
Direct CLAMP-dependent HS-induced Down Loops N=106
CLAMP
Indirect CLAMP-dependent HS-induced Down Loops N=388
Unknown Factor
HS-induced Loop Change Independent N=217
C
Normalized Reads
Ibf1
Ibf2
ISWI
ZIPIC
CP190
Su(Hw)
Pc
-2.0
TSS
TES
2.0Kb
Direct CLAMP-dependent HS-induced Down Loops
Indirect CLAMP-dependent HS-induced Down Loops
HS-induced Loop Change Independent
Random genes
D
chr2L
820
825
830
835
840
845
850 Kb
855
CLAMP
CLAMP-associated HS induced Down-Loops
CP190
ZIPIC
Ibf1
Ibf2
ISWI
Su(Hw)
Pc
Genes
Clp
CG3662
CG3862
dock
drongo
lncRNA:CR44060
CG4291
kraken

Figure 5

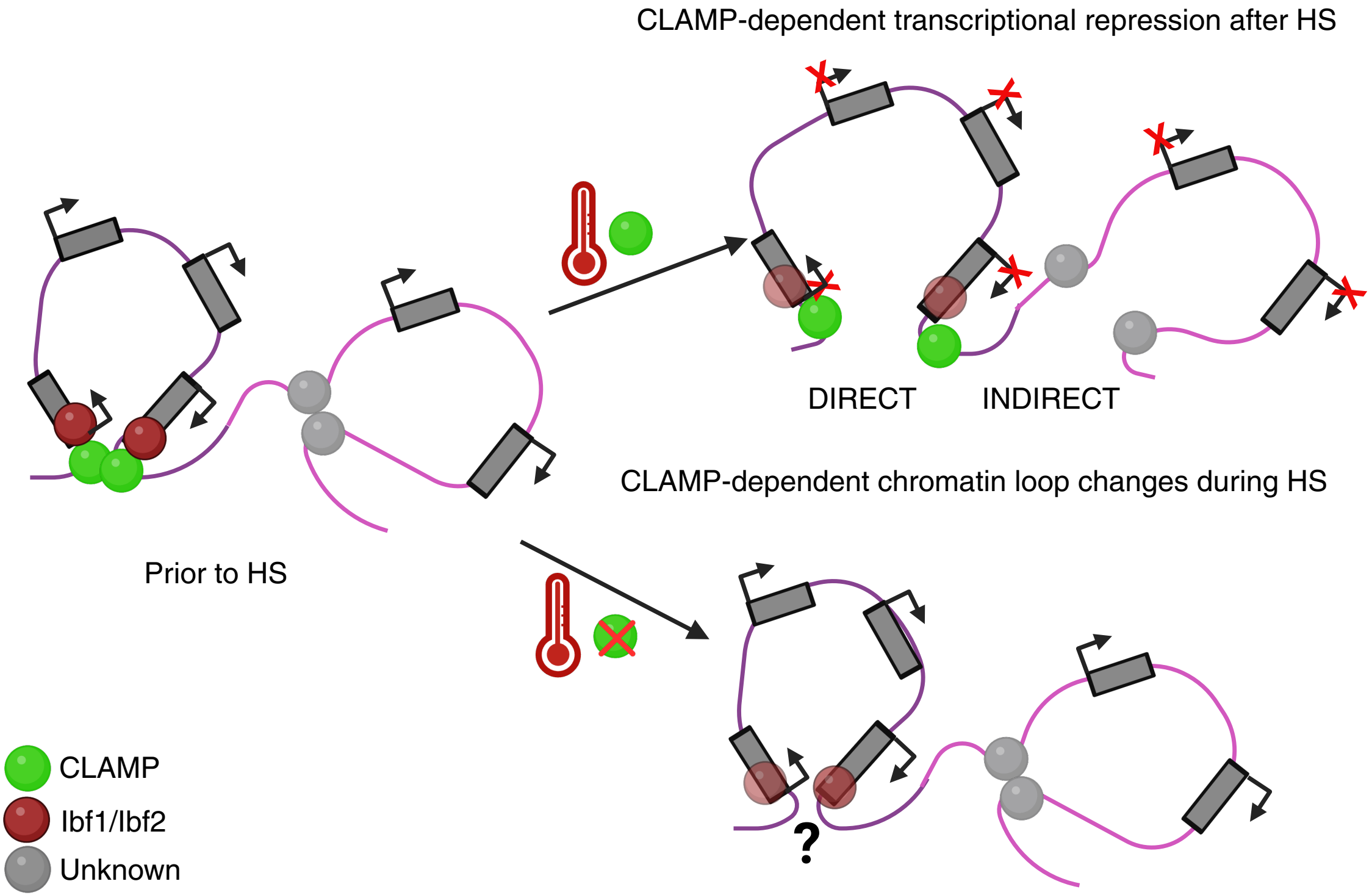
CLAMP-dependent transcriptional repression after HS
DIRECT
INDIRECT
CLAMP-dependent chromatin loop changes during HS
Prior to HS
?
CLAMP
Ibf1/Ibf2
Unknown

Figure 1. CLAMP regulates heat-stress-induced transcriptional repression more strongly than activation

A-B. MA plots showing significant changes (FC ≥ 1.5 and padj ≤ 0.05) in the levels of nascent transcripts (red dots) after HS (heat stress) compared to the control NHS (No heat stress) condition in control (*gfp RNAi*) cells (**A**) and after HS (heat stress) in the absence of CLAMP (*clamp RNAi*) compared to control (*gfp RNAi*) cells (**B**). Dotted horizontal lines in **A** and **B** denote ± 1 $\log_2$ FC change cutoffs.

C. Immunofluorescence images of HS (37ºC for 1 Hr) salivary gland polytene spreads showing the distribution of active RNA polymerase II (red) on chromatin (DAPI: blue) in the presence (undriven *clamp RNAi*) and absence (*fkh-GAL4>clamp RNAi*) of CLAMP (green). The scale bar (100 μM) applies to both panels in **C**.

D-E. Venn diagrams comparing HS-activated transcripts (deep red circle in **D**) and HS-repressed transcripts (light red circle in **E**) from control cells (*gfp RNAi*) to *clamp RNAi* HS Up-regulated (dark green circle) and *clamp RNAi* HS Down-regulated (light green circle) transcripts in *clamp* RNAi-treated cells.

Figure 2. Heat stress induces widespread local 3D chromatin changes at the loop anchors

A-B. MA plots for **differential** loop anchors gained upon HS (HS induced Up loop anchors) or loop anchors lost upon HS (HS induced Down loop anchors) in control cells (**A,** Up loops=24,291, Down Loops=4,265**)** and *clamp RNAi* cells (**B,** Loops Up-regulated=8,274, Loops Down-regulated =2,000**). p<0.01**

C. Barplots show the average number of genes associated with (top box) and present at (bottom box) the HS-induced genome-wide chromatin loop anchors and HS-induced CLAMP-dependent chromatin loop anchors.

D. Box plots showing average loop size of HS-induced genome-wide changing chromatin loops and CLAMP-dependent HS-induced differential chromatin loops with significant difference between average chromatin HS-induced up and down loop sizes, both in case of HS-induced genome-wide changing chromatin loops (Mann–Whitney Test, FDR corrected p=5.63E-186) and

CLAMP-dependent HS-induced differential chromatin loops (Mann–Whitney Test, FDR corrected p=3.97E-70), and also between HS-induced genome-wide changing and CLAMP-dependent HS-induced differential chromatin loops themselves (Mann–Whitney Test, FDR corrected p=0)

E. Upset Plot showing genes associated with differential chromatin loop changes and cardinality of every category combination seen as chromatin loop changes after HS in control (top two rows) and *clamp* RNAi-treated (bottom two rows) cells. The first four columns show chromatin loop-associated genes only in each category, and the following six columns show those in each combination of exactly two named sets, the four columns after that combination of three named sets, and the last column shows genes associated with chromatin loop changes in all four categories. HS-associated CLAMP-dependent chromatin loop changes are mostly represented in the last three columns/bars.

F-I. Venn diagrams comparing HS-associated chromatin loop changes (genes within the loop) and HS-activated and repressed genes (**F** and **G**); as well as CLAMP-dependent chromatin loop changes during HS with CLAMP-dependent HS-induced transcriptional changes (**H** and **I**), showing significant (Fisher's Test) overlap between HS-associated Up loops (**F**) and Down loops (**G**) with HS-repressed genes; and CLAMP-dependent HS-associated Down loops (**H,** *clamp RNAi* up-regulated HS-loops) and Up loops (**I,** *clamp RNAi* down-regulated HS-loops) with CLAMP-dependent HS-repressed genes (*clamp RNAi HS* up-regulated genes). FDR corrected **p-values** are 7.487 E-09 (**F**), 2.53 E-4 (**G**), 2.0 E-6 (**H**), and 4.290 E-15 (**I**), respectively.

J. 350 kb region on 3L showing differential contact interaction results of selfish algorithm on HS and NHS micro-C contact map (**I**) with associated chromatin loops that are formed (**II**) and inhibited after HS (**III**). CLAMP-dependent differential contact interaction results of the selfish algorithm are shown on *clamp* RNAi-treated HS and control HS micro-C contact maps (**IV**) with CLAMP inhibited (**V**) and favoured (**VI**) chromatin loops. The color bar in **I** and **IV** indicates the q-value (BH adjusted *p*-value) produced from the DCI analysis. Darker color means this interaction has a lower q-value; that is to say, two contact maps are more diverse at this location. Bed files for differential nascent RNA-seq (SLAM-seq) data from HS and NHS *clamp* RNAi-treated and control cells show the CLAMP-dependent HS-repressed genes (**VII**) among the corresponding genes within the genomic region associated with the loops (**VIII)**

Figure 3. CLAMP regulates chromatin loop changes during HS, directly as well as indirectly, to repress gene transcription

A. 2D metaplot of CLAMP HiChIP data centered on significant interactions identified from CLAMP HiChIP under NHS or HS conditions for **differential** loop anchors gained upon HS (HS Up loop anchors, N=71) or loop anchors lost upon HS (HS Down loop anchors, N=980). The score indicates the enrichment of the center pixel compared with the top left corner.

B. CLAMP-bound loop pile-ups for HiChIP data from heat stress (HS) and control cells showing loss and gain of chromatin structures marked by chromatin loops defined in HS and control cells. The color is average interaction frequency across the entire dataset surrounding the defined HS Up and Down loops. A high signal indicates strong interaction between loop anchors. ±20 kb padding was applied to the central 2.5 kb bin, displaying a 42.5 kb aggregated region.

C. Barplots showing average number of genes associated within (top box) and present at (bottom box) the CLAMP-bound chromatin loop anchors up and down-regulated after Heat shock (HS)

D. Box plots showing significant difference (Mann–Whitney Test, FDR corrected p=0.0354) between average loop size of CLAMP-bound chromatin loop anchors up and down-regulated after Heat shock (HS).

E-F. Venn diagrams comparing all (Micro-C data) and CLAMP-bound (HiChIP data) chromatin loops lost after HS with HS-repressed (**E**) and CLAMP-dependent HS-repressed genes (**F**), showing significant (Fisher's Test) overlap between CLAMP-bound HS-associated Down-loops with global genome-wide loss of HS-associated loops (p=1.26E-115), HS-repressed genes (p=9.59E-18), and CLAMP-dependent HS-repressed genes (*clamp RNAi HS* up-regulated genes, p=2.57E-19).

G. 300 kb region on 2R showing CLAMP-regulated differential contact interaction results of selfish algorithm on *clamp* RNAi-treated and control HS micro-C contact map (**I**) with associated CLAMP suppressed (**II**) and induced (**III**) chromatin loops after HS. CLAMP-associated differential contact interaction results of the selfish algorithm are shown on HS and NHS CLAMP HiChIP contact maps (**IV**) with CLAMP-bound (**V** and **VII**) directly associated Up (**VI**) and Down (**VIII**) chromatin loops. The color bar in **I** and **IV** indicates the q-value (BH adjusted *p*-value)

produced from the DCI analysis. Darker color means this interaction has a lower q-value; that is to say, two contact maps are more diverse at this location. Normalized reads and bed files for differential nascent RNA-seq (SLAM-seq) data from HS and NHS *clamp* RNAi-treated and control cells show the CLAMP-dependent HS-repressed genes (**IX and X**) among the corresponding genes within the genomic region associated with the loops (**XI)**

Figure 4. HS-associated chromatin loops directly and indirectly regulated by CLAMP have different chromatin-bound factors under NHS conditions

A. Venn diagram comparing all CLAMP-dependent (Micro-C data, *clamp RNAi* up-regulated HS Loops) and CLAMP-bound (HiChIP data) chromatin loops lost after HS with CLAMP-dependent HS-repressed genes, showing significant (Fisher's Test) number of CLAMP-dependent HS-repressed genes are associated with CLAMP-dependent loss of chromatin loops after HS (p=1.55E-04) and a significant proportion of these are directly CLAMP-bound (p=8.78E-32).

B. Schematic showing three categories of CLAMP-dependent HS-repressed genes based on 3D chromatin organisational changes associated with HS.

C. Average profile for chromatin-bound factors across CLAMP-dependent HS-repressed genes present at direct and indirect CLAMP-dependent HS-induced Down-loop anchors, genes not associated with any loop anchors, and a random set of genes (negative control).

D. 35 kb region on 2L showing distribution of chromatin bound factors at CLAMP-dependent HS-repressed genes *dock* and *drongo* and associated CLAMP-bound chromatin loops lost after HS

Figure 5. Model for CLAMP-dependent HS-induced transcriptional gene repression

Figure S1

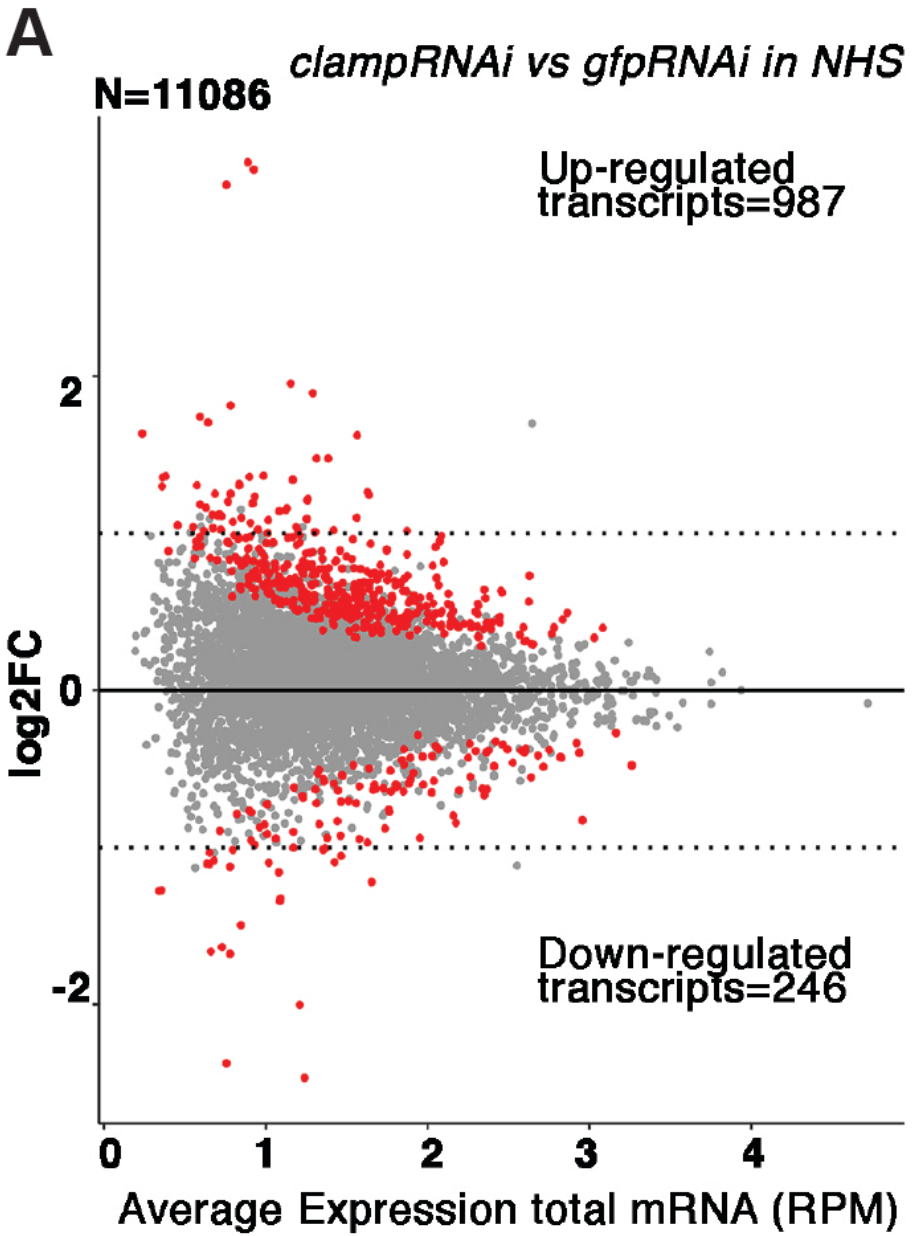
A
clampRNAi vs gfpRNAi in NHS
N=11086
Up-regulated
transcripts=987
Down-regulated
transcripts=246
log2FC
2
0
-2
0
1
2
3
4
Average Expression total mRNA (RPM)

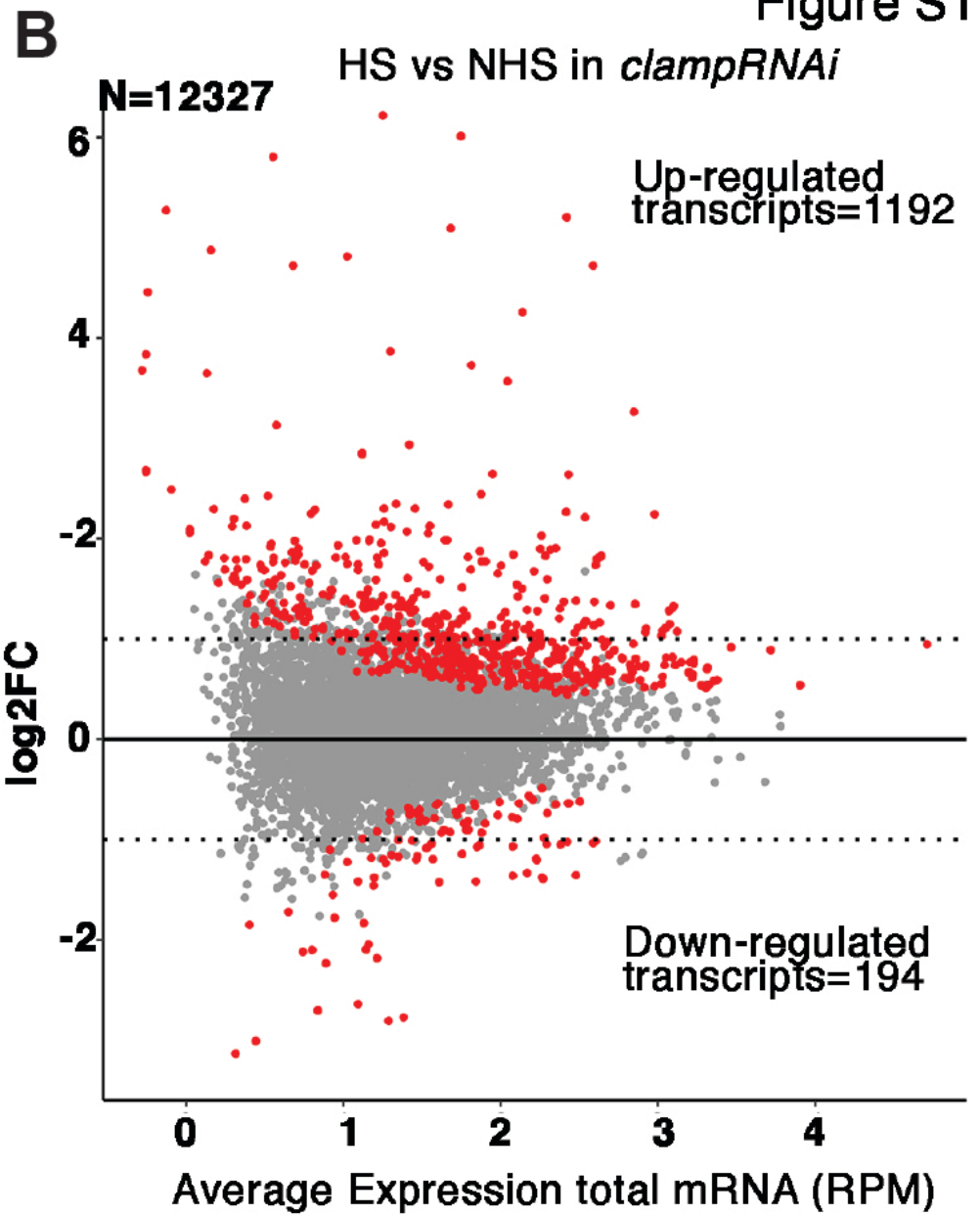
B
HS vs NHS in clampRNAi
N=12327
Up-regulated
transcripts=1192
Down-regulated
transcripts=194
log2FC
6
4
-2
0
-2
0
1
2
3
4
Average Expression total mRNA (RPM)

Figure S2

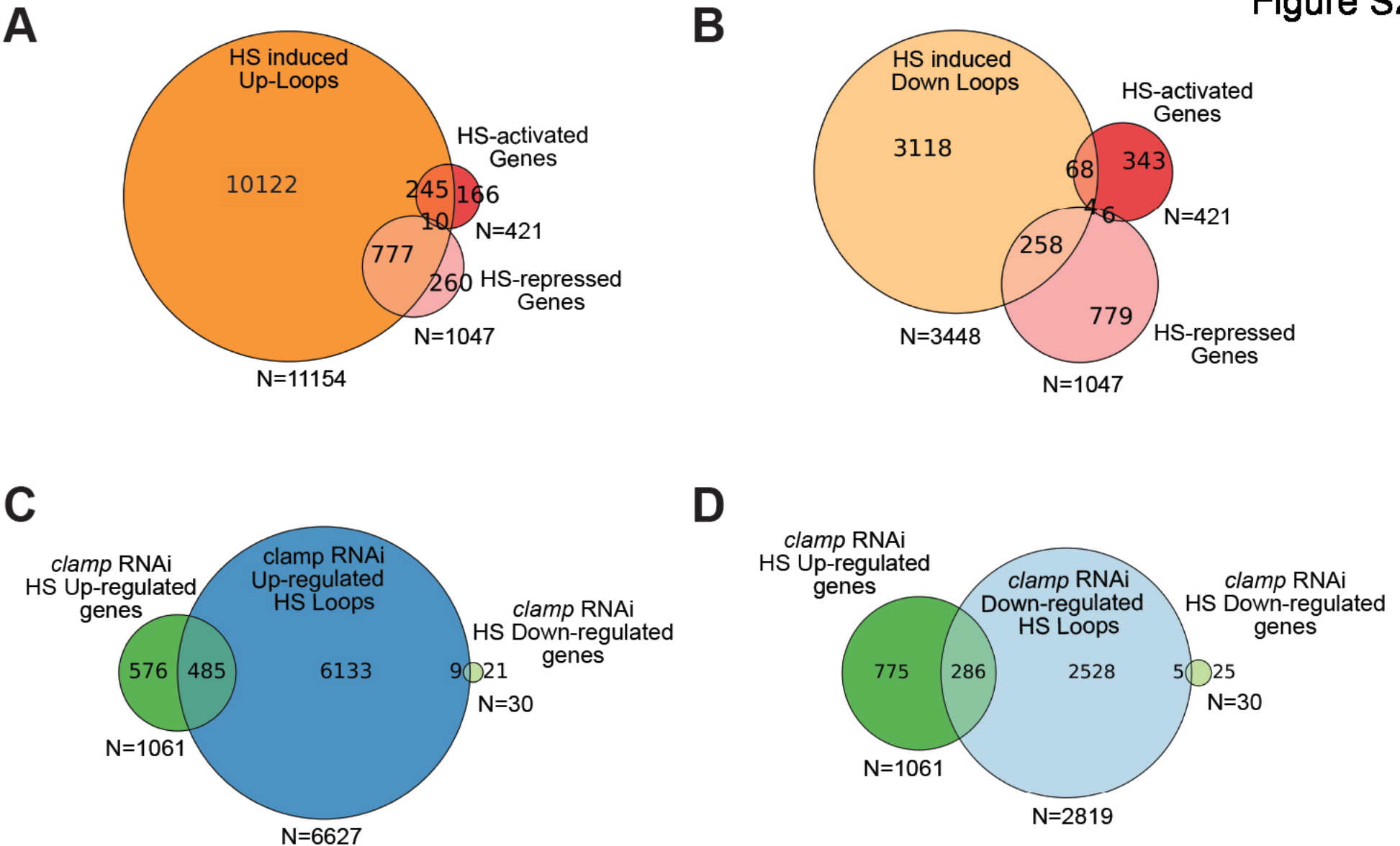
A
HS induced
Up-Loops
10122
HS-activated
Genes
245
166
10
N=421
777
260
HS-repressed
Genes
N=1047
N=11154
B
HS induced
Down Loops
3118
HS-activated
Genes
68
343
4
6
N=421
258
779
N=3448
HS-repressed
Genes
N=1047
C
clamp RNAi
HS Up-regulated
genes
clamp RNAi
Up-regulated
HS Loops
clamp RNAi
HS Down-regulated
genes
576
485
6133
9
21
N=30
N=1061
N=6627
D
clamp RNAi
HS Up-regulated
genes
clamp RNAi
Down-regulated
HS Loops
clamp RNAi
HS Down-regulated
genes
775
286
2528
5
25
N=30
N=1061
N=2819

Figure S3

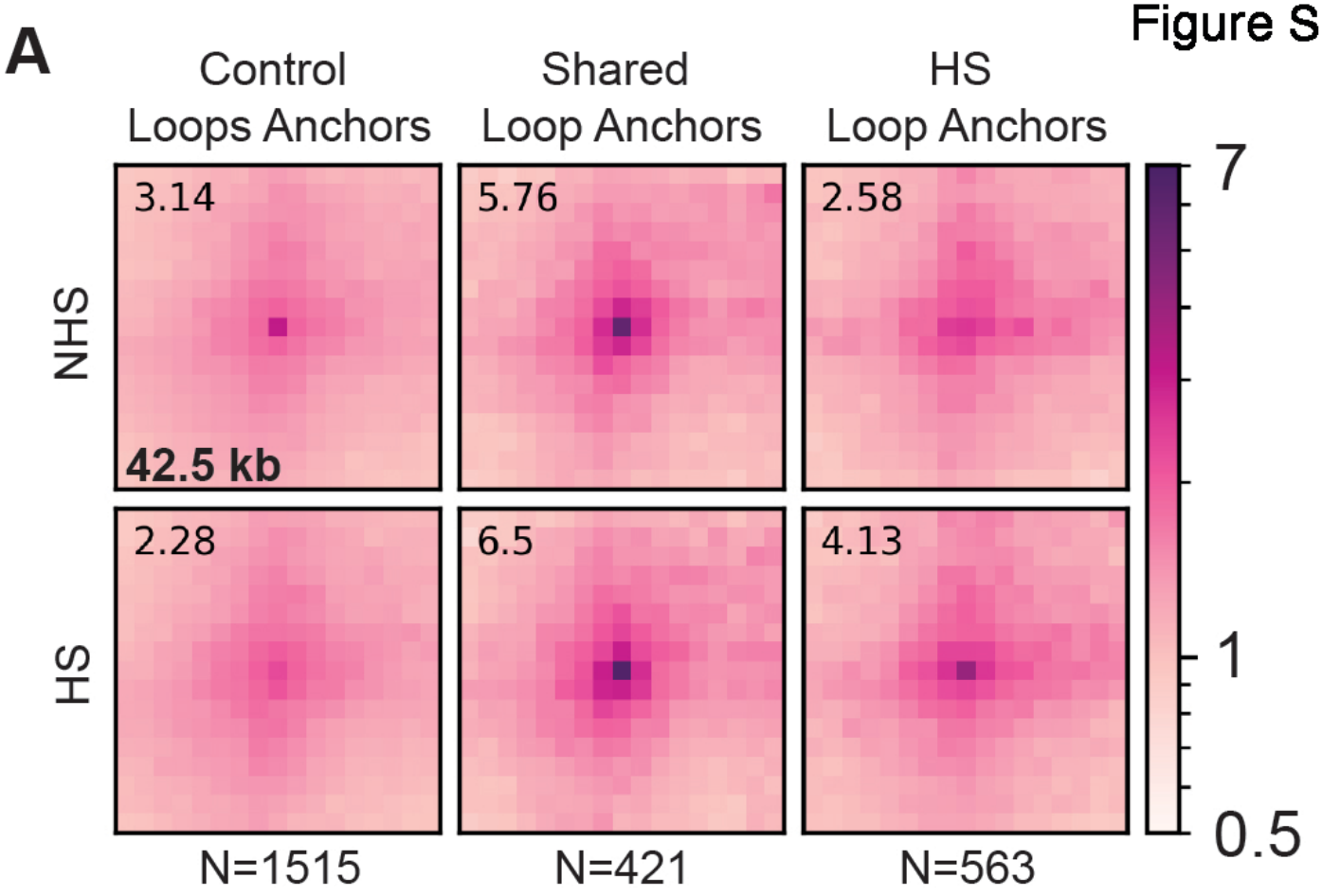
A
Control
Loops Anchors
Shared
Loop Anchors
HS
Loop Anchors
NHS
HS
3.14
5.76
2.58
42.5 kb
2.28
6.5
4.13
N=1515
N=421
N=563
7
1
0.5

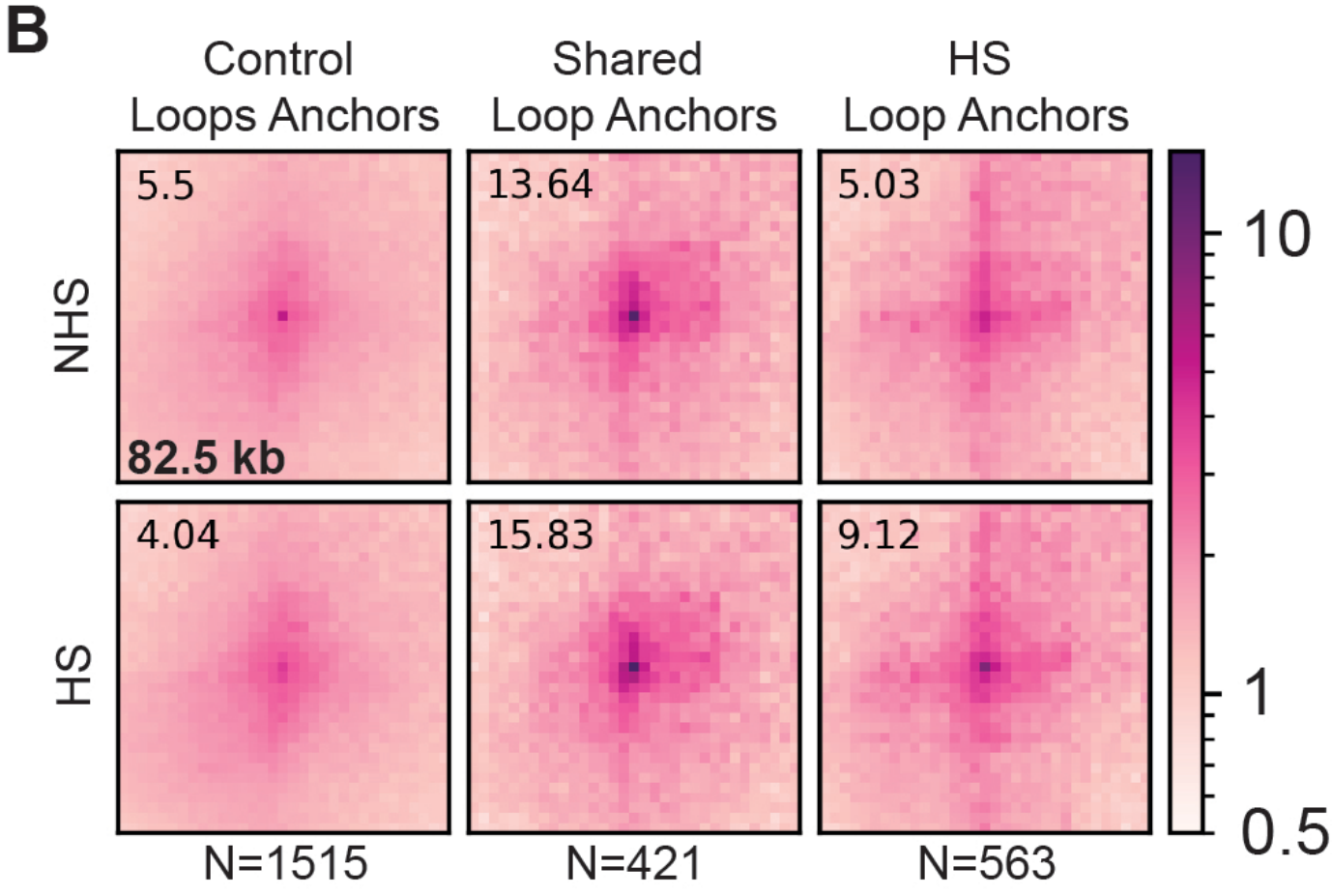
B
Control
Loops Anchors
Shared
Loop Anchors
HS
Loop Anchors
NHS
HS
5.5
13.64
5.03
82.5 kb
4.04
15.83
9.12
N=1515
N=421
N=563
10
1
0.5

Figure S4

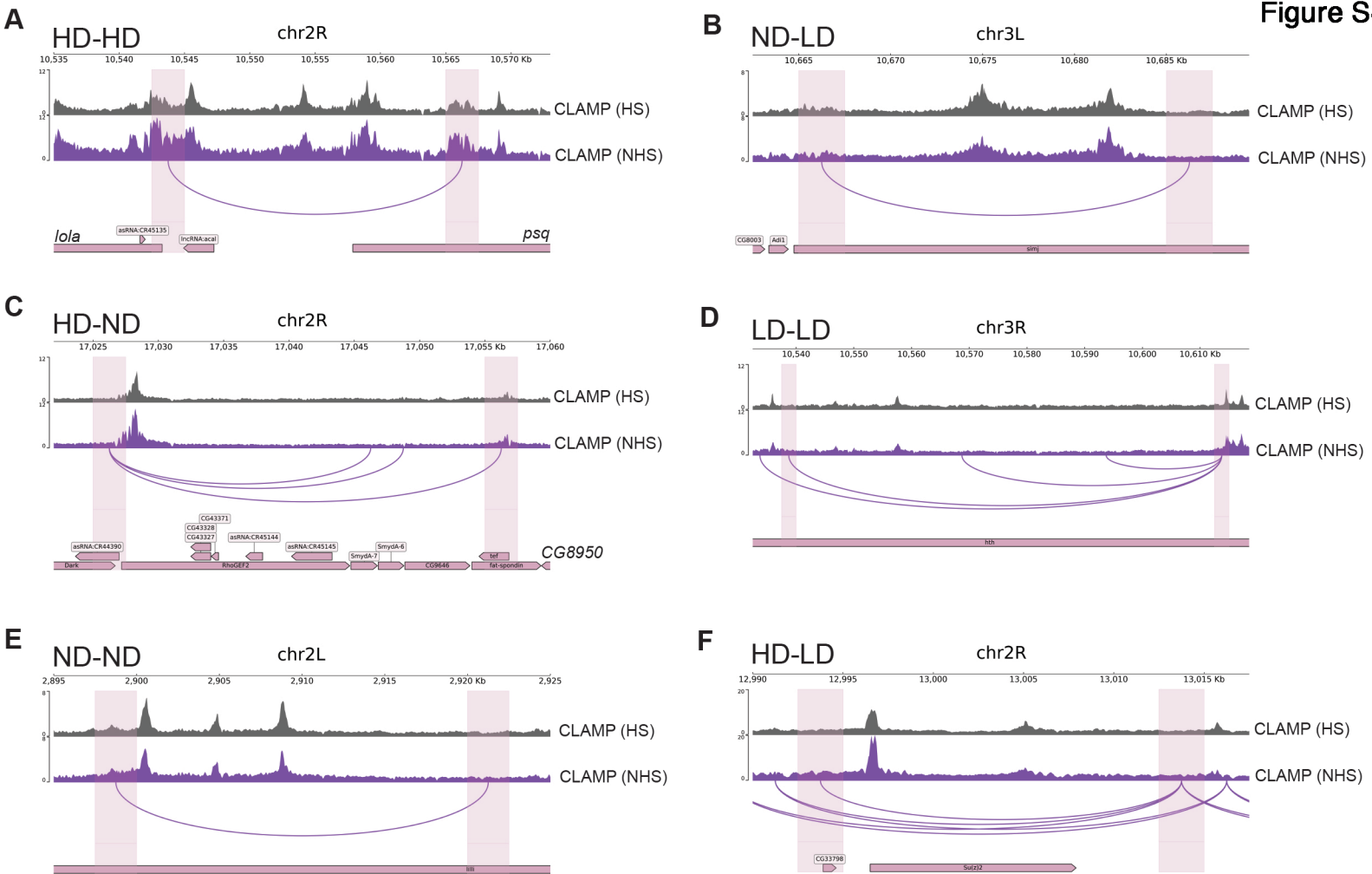
A
HD-HD
chr2R
10,535
10,540
10,545
10,550
10,555
10,560
10,565
10,570 Kb
CLAMP (HS)
CLAMP (NHS)
lola
asRNA:CR45135
lncRNA:acal
psq
B
ND-LD
chr3L
10,665
10,670
10,675
10,680
10,685 Kb
CLAMP (HS)
CLAMP (NHS)
CG8003
Adi1
simj
C
HD-ND
chr2R
17,025
17,030
17,035
17,040
17,045
17,050
17,055 Kb
17,060
CLAMP (HS)
CLAMP (NHS)
CG43371
CG43328
CG43327
asRNA:CR44390
asRNA:CR45144
asRNA:CR45145
SmydA-6
SmydA-7
tef
CG8950
Dark
RhoGEF2
CG9646
fat-spondin
D
LD-LD
chr3R
10,540
10,550
10,560
10,570
10,580
10,590
10,600
10,610 Kb
CLAMP (HS)
CLAMP (NHS)
hth
E
ND-ND
chr2L
2,895
2,900
2,905
2,910
2,915
2,920 Kb
2,925
CLAMP (HS)
CLAMP (NHS)
F
HD-LD
chr2R
12,990
12,995
13,000
13,005
13,010
13,015 Kb
CLAMP (HS)
CLAMP (NHS)
CG33798
Sulf2j2

Supplementary figure legends

Fig. S1 CLAMP functions more frequently as a repressor than an activator in both NHS and HS conditions.

A-B. MA plots show more up-regulated nascent transcripts (positive red dots, $p < 0.05$, log2FC $\geq$ 2) in both *clamp RNAi*-treated cells under NHS (no heat stress) and HS (heat stress) conditions.

Fig. S2 Many CLAMP-dependent repressed genes are present at the loop anchors of CLAMP-dependent HS-associated chromatin loops lost after HS.

A-D. Venn diagrams comparing HS-associated chromatin loop changes (genes at the loop anchors) and HS-activated and repressed genes (**A** and **B**); as well as CLAMP-dependent chromatin loop changes during HS with CLAMP-dependent HS-induced transcriptional changes (**C** and **D**), showing significant (Fisher's Test) overlap between HS-associated Up loops (**A**) and Down loops (**B**) with HS-repressed genes; and CLAMP-dependent HS-associated Down loops (**C,** *clamp RNAi* up-regulated HS-loops) and Up loops (**D,** *clamp RNAi* down-regulated HS-loops) with CLAMP-dependent HS-repressed genes (*clamp RNAi HS* up-regulated genes).

Fig. S3 CLAMP-HiChIP identifies CLAMP-bound chromatin loops in control and HS cells.

A-B APA plots of CLAMP HiChIP loops centered on three classes of significant loop interactions identified by CLAMP HiChIP in both NHS and HS conditions: 1) Loops identified only in NHS conditions (control loops, N=1515); 2) Loops identified in both NHS and HS conditions (shared loops, N=421) and 3) Loops identified only in HS conditions (HS loops, N=563). The value listed indicates the enrichment of the center pixel compared to the background, at ~40 kb (**A**) and ~80 kb (**B**) resolution.

Fig S4. Most CLAMP-associated changes upon heat stress are three-dimensional and not associated with differences in CLAMP occupancy.

A-F. Example tracks for each class of CLAMP-associated loops lost and gained after HS. The grey tracks show the occupancy of CLAMP upon HS, whereas the purple tracks show CLAMP occupancy in normal conditions (NHS). A purple line connects loop anchor endpoints. Highlighted regions correspond to 2.5 kb anchors. The classes of CLAMP-associated loops shown are: **A**) HD-HD, in which there is a change in both three-dimensional contacts and CLAMP occupancy at both ends of the loop anchor upon HS; **B**) ND-LD in which there is a change in 3D contacts and only a slight change in CLAMP occupancy at one of the ends of the loop anchor upon HS; **C**) HD-ND in which there is a change in 3D contacts and occupancy of CLAMP at one end of the loop anchor upon HS; **D**) LD-LD in which there is a change in 3D contacts and only a slight change in CLAMP occupancy at both of the ends of the loop anchor upon HS. **E**) ND-ND in which there is only a change in 3D contacts and no change in CLAMP

occupancy at either end of the loop anchor upon HS; **E**) HD-LD in which there is a change in 3D contact at one end of the loop anchor and only slight change in CLAMP occupancy at another end of the loop anchor upon HS.

Supplementary Table legends

Table S1: List of statistical tests and their results listed for the Venn diagrams generated for analysis of micro-C, HiChIP, and SLAM-seq data sets.

Table S2a-d: List of genes down and up-regulated in control (*gfp RNAi*) cells after HS compared to NHS (a), in *clamp* RNAi-treated cells compared to control (*gfp RNAi*) cells in NHS condition (b), in *clamp* RNAi-treated cells after HS compared to NHS condition (c), and in *clamp* RNAi-treated cells compared to control (*gfp RNAi*) cells under HS condition (d).

Table S3- List of HS-regulated and CLAMP-dependent RNA transcripts from nascent RNA-sequencing SLAM-seq data.

Table S4- List of HS-regulated and CLAMP-dependent genes from nascent RNA-sequencing SLAM-seq data.

Table S5- List of genes present at the loop anchors of the HS up and down loops and those regulated by *clamp* RNAi under HS conditions.

Table S6- List of genes present within the chromatin loops, HS-induced up and down loops, and those regulated by *clamp* RNAi under HS conditions.

Table S7- List of genes present at the loop anchors CLAMP-associated HS-induced up and down loops.

Table S8: List of genes present within CLAMP-associated HS-induced up and down chromatin loops.

Table S9- List of CLAMP-dependent repressed genes which are directly and indirectly regulated by CLAMP at the 3D chromatin structural level after HS.